Memoirs of the Faculty of Engineering, Nagoya University
Vol. 38, No. 1 (1986)

THEORETICAL AND EXPERIMENTAL STUDIES IN EXPRESSION

MOMPEI SHIRATO, TOSHIRO MURASE
and MASASHI IWATA

Department of Chemical Engineering

(Received May 31, 1986)

Abstract

The basic analytical methods for expression, the separation of liquid from solid-liquid systems by compression, are presented from the viewpoint of the flow through compressible porous media. The mathematical models of the Terzaghi model, the Terzaghi-Voigt combined model and a simplified semi-theoretical equation are summarized. On the basis of the theory, constant-pressure expression of both semisolid materials and slurries, and two-dimensional expression on a tubular filter element, are discussed. It is also shown that the constant-rate expression process is well described from calculations based upon constant-pressure expression data. Internal mechanisms of settling sediments are mathematically analysed on the basis of consolidation theory, and the basic differential equations for settling of concentrated suspensions are presented. The hydraulic expression phenomenon in ordinary filter press operation, which depends on a change in filtrate flow pattern, is also described and analyzed.

CONTENTS

Introduction

Expression is the operation of separating liquid from a two-phase solid-liquid system by compression under conditions that allow the liquid to escape while the solid is retained between the compressing surfaces. Expression is distinguished from filtration in that pressure is applied by movement of the retaining walls instead of by pumping the mixture into a fixed chamber. In filtration, the original mixture is sufficiently fluid to be pumpable; in expression the material may appear to be either entirely semisolid or a slurry.

In spite of substantial progress in filtration theory in the past several decades, the theory of expression is far from complete. Most previous experimental work has been done on a particular material and has led only to the development of empirical equations which definitely lack general application.

Gurnham and Masson[1] studied the equilibrium conditions of expression, i. e. the conditions after a constant pressure has been maintained until no further flow occurs. Koo[2] studied the expression of various oil seeds over ranges of pressures, temperatures, pressing times and moisture contents, and presented an empirical equation relating the expressed liquid weight to pressure, time and viscosity, while Nagai and Taguchi[3] attempted to apply filtration theory to expression of fermentation mashes and Körmendy[4] concluded that the pressing time required to achieve the same percent yield of fluid is proportional to the square of the initial thickness of the material to be expressed.

The principal objective of this paper is to present logical analytical methods for practical expression. The paper is composed of six chapters. Chapter 1 deals with the analytical method for constant-pressure expression.[5~7] To analyze the consolidation period, the Terzaghi model and the Terzaghi-Voigt combined model

are introduced. Chapter 2 gives a simplified computation method for constant-pressure expression.[8,9] Mathematical solutions for constant-pressure expression based upon the Terzaghi and the Terzaghi-Voigt models are simplified and a semi-theoretical expression equation is presented for practical convenience in data analysis in industry. Chapter 3 is concerned with two-dimensional expression under constant pressure.[10] The two-dimensional expression problem can be solved by use of the effective consolidation area factor. Chapter 4 deals with constant-rate expression,which is often encountered industrially.[11] The previous analytical method for constant-pressure expression is extended to expression under variable-pressure conditions. Chapter 5 presents a method for analyzing the settling of thick slurries due to consolidation.[12] A useful method for obtaining compression-permeability characteristics of sediments is also discussed. Chapter 6 is concerned with hydraulic expression.[13,14] Filtration-consolidation phenomena due to the change in filtrate flow pattern are described in detail.

1. Theory of Constant-Pressure Expression

According to the variation of expression pressure and flow rate with time, expression (like filtration) can be classified into the three categories of constant-pressure,[5~9] constant-rate,[11,15] and variable-pressure, variable-rate[15] expression. In this chapter, theories regarding constant-pressure expression will be discussed.

Fig. 1. 1 shows the assembled view of one of the compression permeability cells used to study dewatering rates of filter cakes during constant-pressure expression. To investigate the correlation between theories and experiments, various kinds of materials are used.

In expression experiments under constant-pressure conditions, the solid-liquid mixture is introduced into a cell-cylinder and a constant mechanical pressure is applied to the piston. Liquid squeezed from the mixture is allowed to drain from either the upper side or from both the top and bottom drainage surfaces, and time, θ, vs. thickness of compressed mixture, L, is recorded.

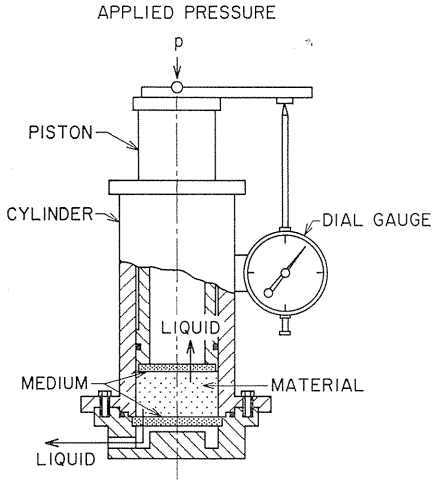

Fig. 1. 1. Compression permeability cell.

In dealing with the mathematics of expression, the operation should be divided into two parts in view of the mechanism of flow through porous media. In the first part, the flow mechanism is actually filtration; in the second part, the mechanism is so-called consolidation.

In general, the original mixture to be expressed may be thick, and may appear to be a semisolid or slurry. Provided the original mixture in the cell is virtually a slurry, applying mechanical pressure to the piston causes a sudden, uniform increase of hydraulic pressure through the slurry up to the same pressure as that applied, and expression may proceed on the principle

of filtration at constant pressure.

1. 1. Filtration period

A schematic picture of the filtration period is shown at the left in Fig. 1. 2. Filtration will terminate in consolidation when the whole slurry forms filter cakes, as shown at the right in Fig. 1. 2. By means of a mass balance, it is possible to calculate the maximum filter cake thickness L_1 in accord with Eq. (1. 1).

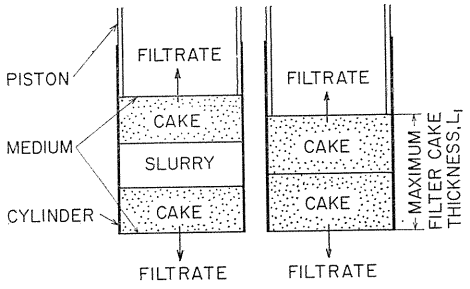

Fig. 1. 2. Schematic picture for filtration period.

$$L_1=\left(\frac{m-1}{\rho}+\frac{1}{\rho_s}\right)\rho_s\omega_0 \qquad (1.1)$$

In Eq. (1. 1), ω_0 represents the total volume of dry solids per unit sectional area, ρ the density of liquid, ρ_s the true density of solids, and m the ratio of wet to dry filter cake mass. The maximum filter cake thickness L_1 is the transition point from filtration to consolidation.

In Fig. 1. 3, expression data for Hara-Gairome clay — Solka-Floc mixture are shown. The thickness of the mixture in the cell is plotted against the expression time. In these plots the transition point L_1 from filtration to consolidation is not quite clear. However, the transition point L_1 can be easily determined by a graphical method, as illustrated in Fig. 1. 4.

As shown in Fig. 1. 4, it is apparent from both theoretical and experimental points of view that $-\Delta L/\Delta\sqrt{\theta+\theta_m}$ is constant for constant-pressure filtration if Ruth's filtration equation holds true, where θ is the expression time and θ_m is the fictitious time of filtration which accounts for the medium resistance. As illustrated in Fig. 1. 4, graphical determination of the transition point is rather simple

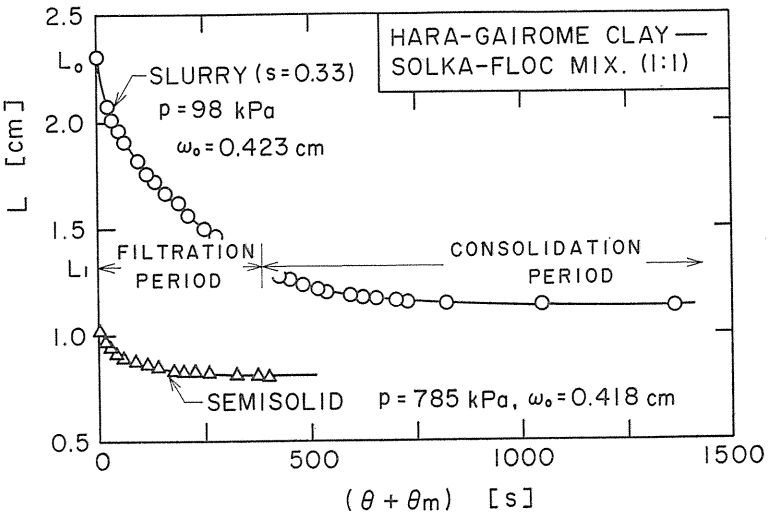

Fig. 1. 3. Experimental results under constant-pressure expression. Thickness of mixture, L, vs. expression time, θ.

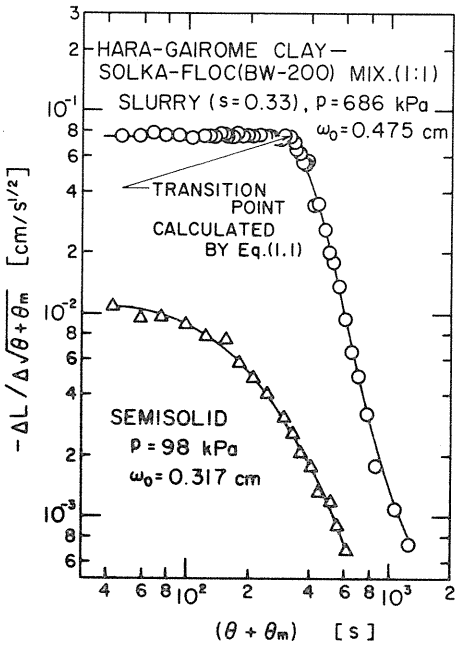

Fig. 1. 4. Determination of transition point between filtration and consolidation periods.

and very accurate. We shall also rely on a calculation using Eq. (1. 1) and assuming the value of m to be known. As may be seen in Fig. 1. 4, the experimentally determined transition point and the theoretically calculated one showed remarkable coincidence.

When the solid concentration in the original mixture exceeds a limiting value, the mixture passes into a semisolid state and the filtration portion of the operation disappears. Then the graph of $-\Delta L/\Delta\sqrt{\theta+\theta_m}$ has no horizontal portion, as shown by the lower curve in the graph. This critical value of concentration is equal to the solid concentration of a sediment deposited from a slurry at zero pressure. The porosity corresponding to the critical slurry concentration is equal to the porosity ε_i of the surface layer of a filter cake. Therefore, the critical concentration is a property of the material itself.

To derive the fundamental mathematical equations for expression, we begin with Ruth's filtration equation in the form

$$\frac{dv_f}{d\theta_f}=\frac{p(1-ms)}{\mu\alpha_{av}\rho s(v_f+v_m)} \tag{1.2}$$

where θ_f is the filtration time.

The filtrate volume v_f-time θ_f relation at a constant pressure is represented by Eq. (1. 3), because the average specific resistance α_{av} and the ratio m of wet to dry cake mass are virtually constant.

$$(v_f+v_m)^2=K(\theta_f+\theta_m) \tag{1.3}$$

By using the thickness L of the mixture under compression instead of the filtrate volume v_f, Eq. (1. 3) may be rewritten as

$$(L_0-L)+L_m=i\{K(\theta_f+\theta_m)\}^{1/2} \tag{1.4}$$

where L_0 is the initial thickness of the mixture and i is the number of drainage surfaces. The value L_m is numerically equal to the fictitious filtrate volume iv_m which accounts for the medium resistance.

Dividing Eq. (1. 4) by $(L_0-L_1)=(1-ms)\rho_s\omega_0/\rho s$ and defining a filtration ratio U_f, a filtration time factor T_f and a modified filtration coefficient K_w yields a very simple form:[5,6]

$$(U_f+U_m)=(T_f+T_m)^{1/2} \tag{1.5}$$

where

$$U_f=\frac{L_0-L}{L_0-L_1},\quad U_m=\frac{L_m}{L_0-L_1} \tag{1.6}$$

$$T_f=\frac{i^2K_w\theta_f}{\omega_0{}^2},\quad T_m=\frac{i^2K_w\theta_m}{\omega_0{}^2} \tag{1.7}$$

$$K_w=K\frac{\rho^2s^2}{\rho_s{}^2(1-ms)^2}=\frac{2p}{\mu\alpha_{av}\rho_s{}^2}\frac{\rho s}{1-ms} \tag{1.8}$$

In these equations, s represents the concentration of the mixture, and K the so-called filtration coefficient at constant pressure. By using the relation $\theta_m=\omega_0{}^2U_m{}^2/i^2K_w$ of fictitious filtration time, Eq. (1.5) can be rewritten as

$$U_f=\frac{i\sqrt{K_w}}{\omega_0}(\sqrt{\theta_f+\theta_m}-\sqrt{\theta_m}) \tag{1.9}$$

It is apparent that the filtration ratio U_f equals zero at the beginning of expression when the load is applied and that it increases gradually to one in accordance with the progress of filtration. These equations are the basic formulas for obtaining solutions of the filtration period of constant-pressure expression.

In accordance with the theory indicated by Eqs. (1.5) and (1.9),we find a unique linear relationship between U_f and $i(\sqrt{\theta_f+\theta_m}-\sqrt{\theta_m})/\omega_0$ as illustrated in Fig. 1.5. It is now apparent from both theoretical and experimental points of view that the time for filtration period is exactly proportional to the square of the solids volume ω_0 in the original solid-liquid mixture.

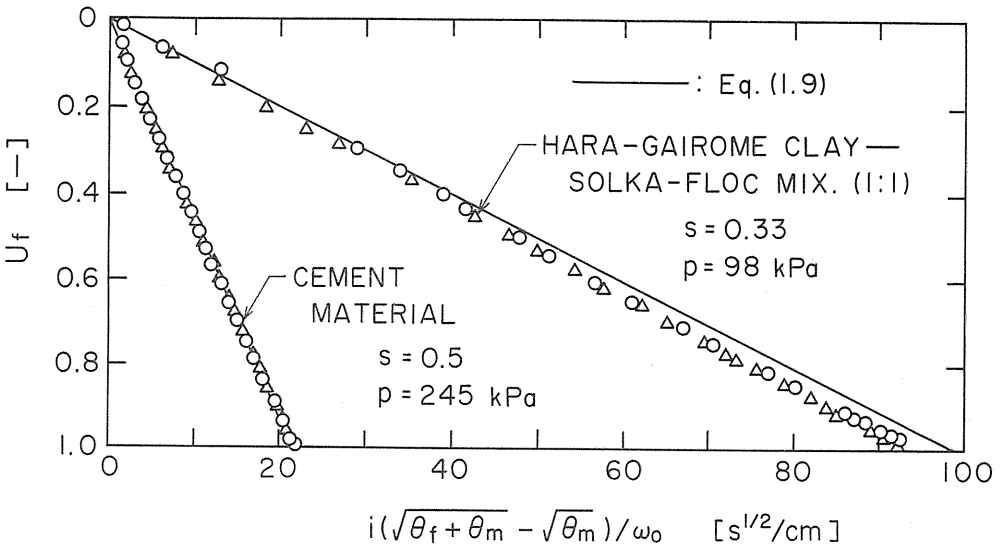

Fig. 1. 5. Filtration ratio, U_f, vs. $i(\sqrt{\theta_f+\theta_m}-\sqrt{\theta_m})/\omega_0$.

1. 2. Consolidation period

When L decreases to a definite thickness L_1, the filtration period ends and further expression proceeds on the principle of consolidation.

Generally, the consolidation period starts after the filtration period, the transition point being L_1. Dehydration by consolidation is distinguished from dehydration by filtration by the fact that the hydraulic pressure in a compressed cake decreases continuously, whereas that in a constant-pressure filter cake is maintained substantially constant. Even when the hydraulic pressure throughout compressed cake becomes zero, a further small decrease in thickness of the compressed cake occurs because of secondary consolidation. The secondary consolidation continues at a speed which depends on the plastic characteristics of the solids.

When the original concentration of a solid-liquid mixture is larger than the critical value, applying a load to the mixture develops an approximately uniform distribution of hydraulic pressure which is lower than the applied pressure, and cake compaction proceeds on the principle of consolidation theory.

1. 2. 1. Terzaghi model

The process of consolidation may be better understood by reference to the famous piston-spring analogy of Dr. Terzaghi[16] in the field of soil mechanics, as shown in Fig. 1. 6. In (a), a spring is immersed in a cylinder of unit sectional area filled with water. In (b), a frictionless piston has been placed in the cylinder and loaded with a load p. As the piston is provided with a closed stopcock, the piston cannot descend and the liquid pressure p_L is equal to the applied pressure p.

Now suppose the stopcock is opened. As the water escapes, the piston sinks lower and lower. At (c) in Fig. 1. 6 the liquid pressure is p_L and the spring carries the load p_s, which is equal to $(p-p_L)$. Sketch (d) represents the final equilibrium condition. Water no longer escapes and the piston ceases to sink. At

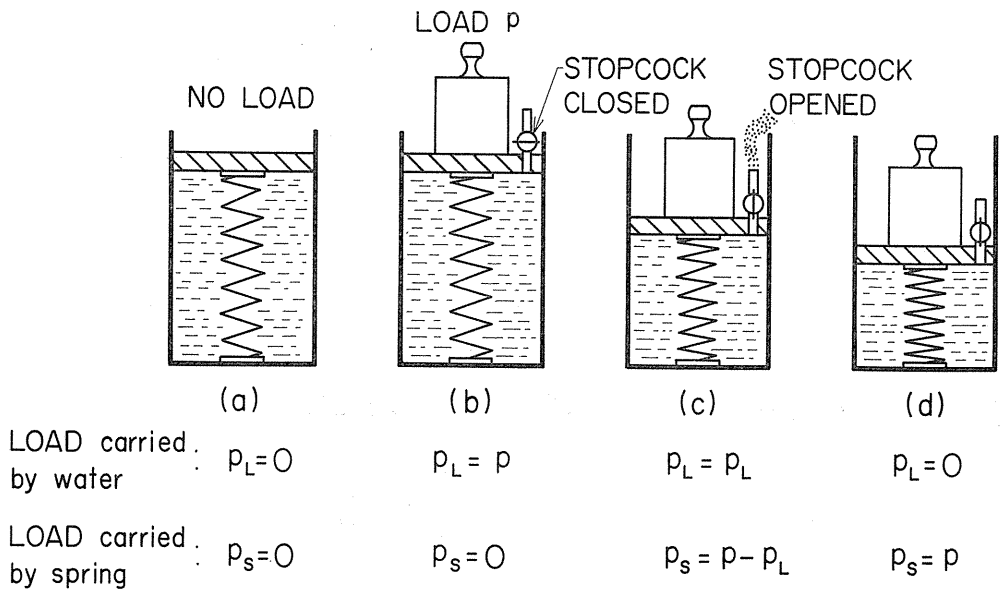

Fig. 1. 6. Schematic picture of Terzaghi model.

this time, the spring must be carrying the total load p and the liquid pressure becomes zero.

In this mechanical analogy, the spring represents the solid particles and the water in the cylinder represents the liquid in voids. The spring force is analogous to the solid compressive pressure p_s.

The one important detail in which this analogy fails to agree with the process of expression is that pressure conditions are the same throughout the height of the cylinder, whereas expression of a solid-liquid mixture begins at the top and bottom drainage surfaces and gradually progresses inward, resulting in uniformly compressed cake of very low moisture content.

To derive the equation for the consolidation period, we begin with the basic equation of flow through porous media. In the conventional Terzaghi theory of consolidation, the x-coordinate distance has been used exclusively, as shown at the left in Fig. 1. 7. However, not only the liquid but also solid particles in an infinitesimal thickness of layer dx at a distance x measured from the septum do move towards the drainage surface, in accord with the progress of consolidation. Consequently, to derive the consolidation equations it is definitely more convenient and more accurate to use solid particle distribution ω instead of the x-coordinate, as shown at the right in Fig. 1. 7, where ω is a moving plane which contains ω m^3/m^2 of solids between the plane and the septum.

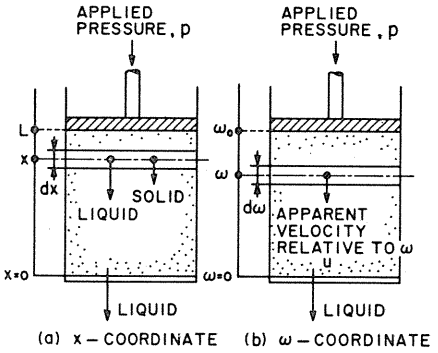

Fig. 1. 7. Schematic picture of cake under consolidation.

The apparent velocity of liquid u viewed from the ω-plane can be represented by

$$u=\frac{1}{\mu\alpha\rho_s}\frac{\partial p_L}{\partial\omega}=-\frac{1}{\mu\alpha\rho_s}\frac{\partial p_s}{\partial\omega} \tag{1.10}$$

The mass balance of liquid in the layer leads to the continuity equation in the form

$$\frac{\partial e}{\partial\theta_c}=\frac{\partial u}{\partial\omega} \tag{1.11}$$

where e is the local value of void ratio and θ_c is the consolidation time.

Combining Eq. (1. 10) with Eq. (1. 11) yields the well-known form of the Diffusion Equation[5]

$$\partial p_s/\partial\theta_c=C_e(\partial^2 p_s/\partial\omega^2) \tag{1.12}$$

where C_e is the so-called modified consolidation coefficient defined by Eq. (1. 13).

$$C_e=1/\{\mu\alpha\rho_s(-de/dp_s)\} \tag{1.13}$$

Eq. (1. 12) is similar to Terzaghi's basic consolidation equation[16] in soil

mechanics with spatial fixed coordinate. It should be noted, however, that Eq. (1. 12) can be used even in the case of a large strain,[17] leading us to a rigorous analytical solution provided the change in C_e-value is not so large, while Terzaghi's basic consolidation equation is applicable only within an infinitesimal strain range. As far as the expression experiments attempted in this study are concerned, the change in C_e-value was not so large when the stages of filtration and consolidation were clearly treated separately.

To obtain the solution of Eq. (1. 12), it is essential to know the inital condition, specifically the hydraulic pressure p_L-distributions in expression materials. The hydraulic pressure distributions in filter cakes of moderate compressibility can approximate a sinusoidal curve.[18]

Then, the mathematical solution for Eq. (1. 12) in the case of a constant-pressure expression of filter cake is given by Eq. (1. 14):[5,6]

$$U_c=(L_1-L)/(L_1-L_\infty)=1-exp(-\pi^2 T_c/4) \tag{1.14}$$

where U_c indicates the so-called average consolidation ratio, and L_1, L and L_∞ are the thickness of materials at $\theta_c=0$, θ_c and ∞, respectively. T_c is the consolidation time factor defined by Eq. (1. 15):

$$T_c=i^2 C_e \theta_c/{\omega_0}^2 \tag{1.15}$$

The mathematical solution for Eq. (1. 12) in the case of a constant-pressure expression of homogeneous semisolid materials is given by Eq. (1. 16):

$$U_c=\frac{L_1-L}{L_1-L_\infty}=1-\sum_{N=1}^{\infty}\frac{8}{(2N-1)^2\pi^2}\,exp\left\{-\frac{(2N-1)^2\pi^2}{4}T_c\right\} \tag{1.16}$$

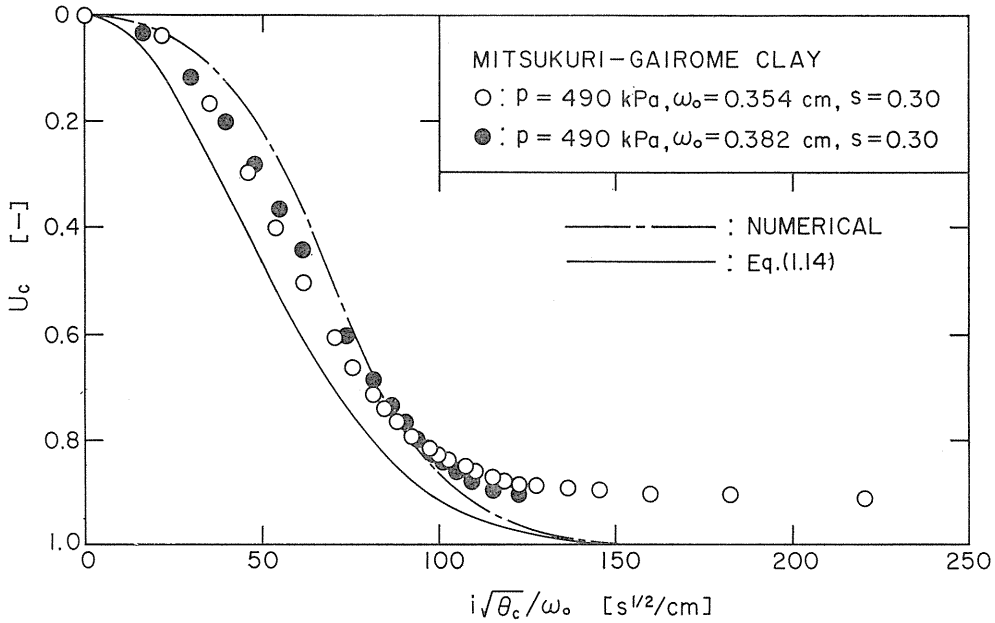

Fig. 1. 8. Constant-pressure expression of Mitsukuri-Gairome clay filter cakes. Average consolidation ratio, U_c, vs. $i\sqrt{\theta_c}/\omega_0$.

or by[19]

$$U_c=\frac{L_1-L}{L_1-L_\infty}=\sqrt{\frac{4}{\pi}T_c}+\sqrt{\frac{4}{\pi}\frac{i^2C_e}{\omega_c{}^2}}\sum_{N=1}^{\infty}(-1)^N\int_0^{\theta_c}\frac{exp\left(-\frac{N^2}{T_c}\right)}{\sqrt{\theta_0}}d\theta_c \quad (1.17)$$

Figs. 1. 8 and 1. 9 compare the experimental data for consolidation of a Mitsukuri-Gairome clay filter cake and a homogeneous semisolid Korean kaolin with calculations based upon Eqs. (1. 14) and (1. 16), respectively. The agreement is rather poor, although the calculated U_c vs. $i\sqrt{\theta_c}/\omega_0$ curves are similar in shape to the experimental curves. In Fig. 1. 9, $e_{1\cdot av}$ is the initial average void ratio of semisolid material.

In view of variations of C_e, Eqs. (1. 10) and (1. 11) are solved numerically[20] by the Runge-Kutta-Gill method, and the results are illustrated in Fig. 1. 8 by a dot-dash line. The agreement is still poor.

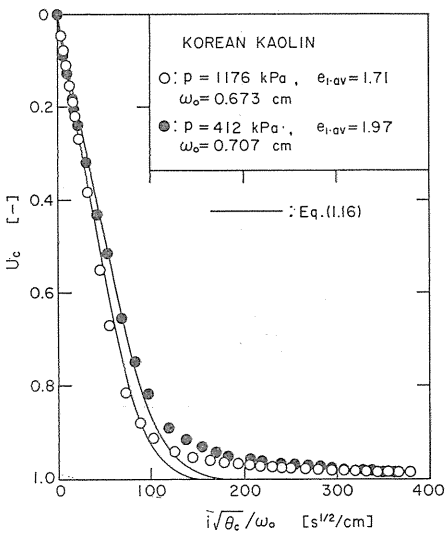

Fig. 1. 9. Constant-pressure expression of semisolid Korean kaolin. Average consolidation ratio, U_c, vs. $i\sqrt{\theta_c}/\omega_0$.

Modified consolidation coefficient C_e

The most important variable C_e can be easily determined by the "fitting method" in view of the similarity in shape of the theoretical U_c-curve and experimental observations. The two curves shown in Fig. 1. 10 represent theoretical calculations based upon the approximate solutions (1. 14) and (1. 16). By the fitting method, θ_{90}, the consolidation time required for attaining 90% of U_c, may be read from experimental data, and C_e is calculated from the following equations (1. 18) and (1. 19), as shown in Figs. 1. 11 and 1. 12.

$$C_e=0.933\omega_0{}^2/i^2\theta_{90} \quad (1.18)$$

$$C_e=0.848\omega_0{}^2/i^2\theta_{90} \quad (1.19)$$

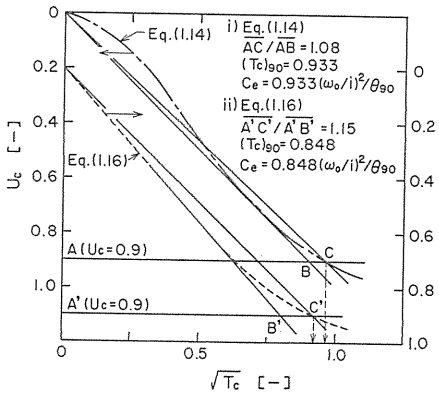

Fig. 1. 10. Fitting method for determining experimental C_e-value.

When θ_{90} is known, the final thickness L_∞ of consolidated mixture is calculated.

C_e can also be calculated in another way, from the compression permeability data. In Fig. 1. 13 the data obtained from compression permeability measurements are shown. At the left the variation of specific resistance α with solid compressive pressure p_s is shown and at the right the variation of void ratio e with p_s is shown for different solids. Compression

permeability data of α and e can be represented in the following form.

$$\alpha=\alpha_0+\alpha_1 p_s^n \text{ : Ruth's form} \tag{1.20}$$

$$e=e_0-C_c ln p_s \text{ : Terzaghi \& Peck's form} \tag{1.21}$$

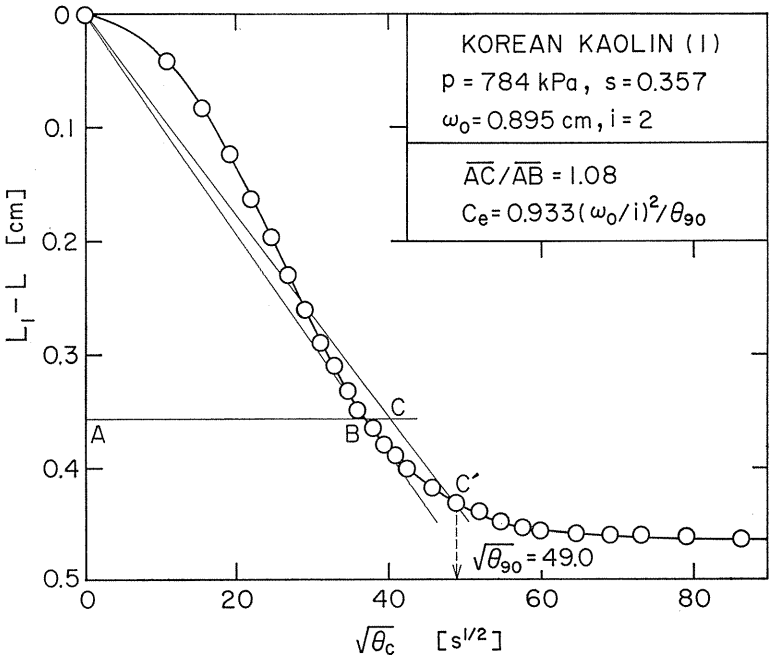

Fig. 1. 11. Fitting method for filter cake consolidation.

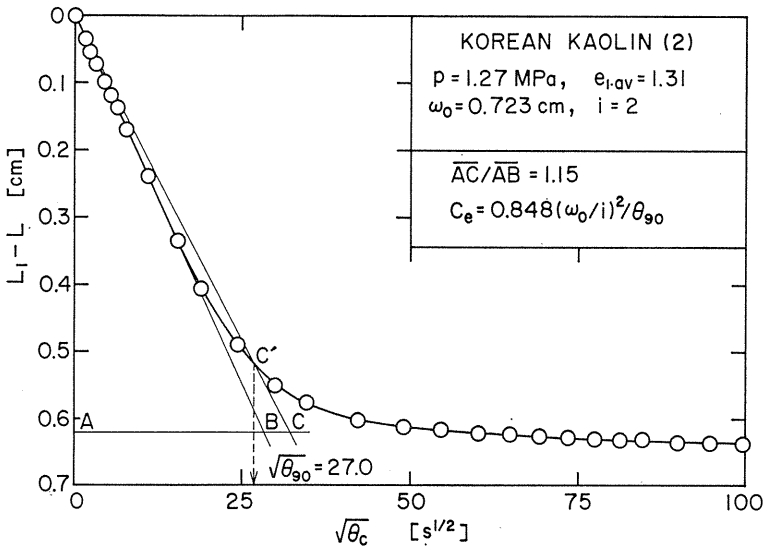

Fig. 1. 12. Fitting method for semisolid consolidation.

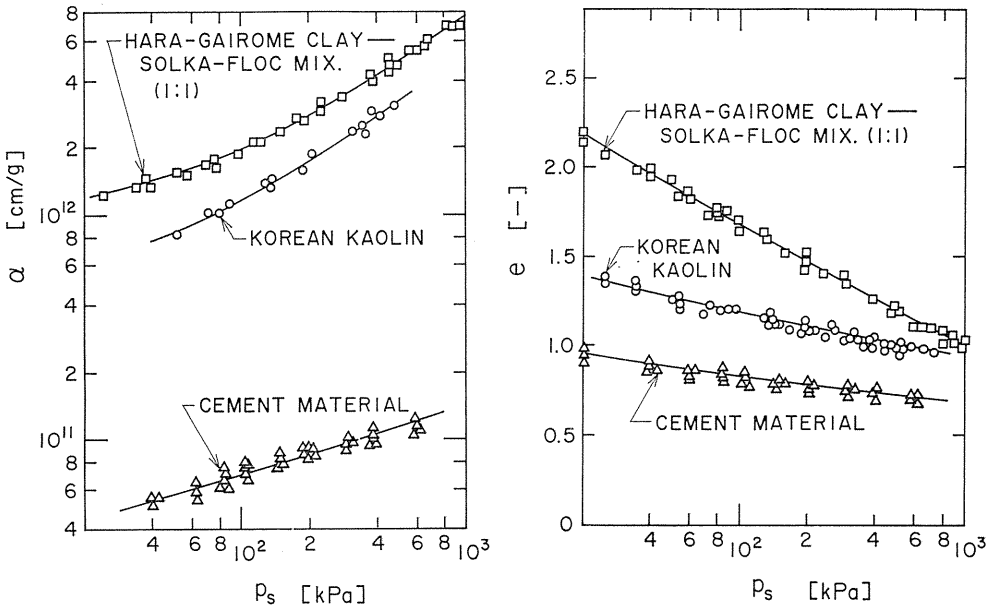

Fig. 1. 13. Compression permeability cell data. Specific resistance, α, and void ratio, e, vs. solid compressive pressure, p_s.

Using the empirical equation of (1. 20) for specific resistance α and Eq. (1. 21) for void ratio e, both obtained from Fig. 1. 13, one can derive the following equation for the modified average consolidation coefficient C_e.

$$C_e=\frac{p_{s\cdot av}}{\mu\rho_s C_c(\alpha_0+\alpha_1 {p_{s\cdot av}}^n)} \tag{1. 22}$$

where $p_{s\cdot av}$ denotes the average solid compressive pressure, which is the arithmetic mean value of the initial average solid compressive pressure $p_s(e_{1\cdot av})$ and the applied expression pressure p.

Essentially, Eq. (1. 22) affords a prediction of C_e, and thus one can theoretically predict the consolidation process from calculations based upon data of compression permeability measurements.

1. 2. 2. Terzaghi-Voight combined model

In the previous section, local void ratio e during the consolidation period was dependent only upon local compressive pressure p_s, and the so-called creep effect was neglected. To obtain more rigorous equations of consolidation, the creep effect of secondary consolidation should be taken into account.

Since the variation of e is caused by both the change in local compressive pressure p_s and the simultaneous effect of creep of solids, e is not a single-valued function of p_s, but is a function of both p_s and time θ_c. Then the mass balance of liquid in an infinitesimal layer of consolidated cake leads to a continuity equation in the form[7,21]

$$\frac{\partial e}{\partial \theta_c}=\left(\frac{\partial e}{\partial \theta_c}\right)_E+\left(\frac{\partial e}{\partial \theta_c}\right)_C=\frac{\partial u}{\partial \omega} \tag{1. 23}$$

In Eq. (1.23), the term $(\partial e/\partial\theta_c)_E$ represents the time rate of change in e due to the so-called primary consolidation and depends only upon the change in p_s. Therefore, the term $(\partial e/\partial\theta_c)_E$ can be rewritten as

$$\left(\frac{\partial e}{\partial\theta_c}\right)_E=\left(\frac{\partial e}{\partial p_s}\right)_E\left(\frac{\partial p_s}{\partial\theta_c}\right)=-a_E\left(\frac{\partial p_s}{\partial\theta_c}\right) \tag{1.24}$$

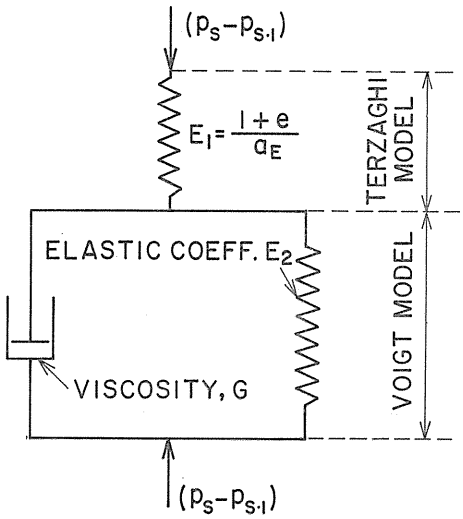

Fig. 1. 14. Schematic picture of Terzaghi-Voigt combined model.

where a_E is the coefficient of compressibility defined by $a_E=-(\partial e/\partial p_s)_E$.

The second term $(\partial e/\partial\theta_c)_C$ in Eq. (1.23), which accounts for the secondary consolidation, is not a single function of p_s, but is a function of both p_s and θ_c.

On the assumption that the rheological constitution of the secondary consolidation is constructed by the Voigt element shown in Fig. 1. 14, the term $(\partial e/\partial\theta_c)_C$ can be given by[21]

$$\left(\frac{\partial e}{\partial\theta_c}\right)_C=-\frac{\partial}{\partial\theta_c}\int_0^{\theta_c}a_c[1-exp\{1-\eta(\theta_c-\tau)\}]\frac{\partial p_s}{\partial\tau}d\tau \tag{1.25}$$

where $a_C=(1+e)/E_2$, $\eta=E_2/G$, E_2 is the elastic coefficient of the spring, G is the viscosity of the dash pot of Voigt's model, and τ is a dummy variable representing an arbitrary consolidation time up to a given elapsed time θ_c.

Substituting Eqs. (1.10), (1.24) and (1.25) into Eq. (1.23), one obtains the consolidation Eq. (1.26) in the form[7,21]

$$\frac{\partial p_s}{\partial\theta_c}+\frac{a_C}{a_E}\frac{\eta\partial}{\partial\theta_c}\int_0^{\theta_c}(p_s-p_{s\cdot1})\,exp\,\{-\eta(\theta_c-\tau)\}d\tau=C_e\frac{\partial^2 p_s}{\partial\omega^2} \tag{1.26}$$

where $p_{s\cdot1}$ is the local value of p_s of the material when $\theta_c=0$. C_e represents the modified consolidation coefficient defined by

$$C_e=\frac{1}{\mu\rho_s\alpha_{av}a_E} \tag{1.27}$$

and is assumed to be a constant in Eq. (1.26); and α_{av} in Eq. (1.27) is the average specific resistance of cake during consolidation and is assumed to be constant.

The analytical solutions of the consolidation equation based upon the Terzaghi-Voigt model are given by

$$U_c=\frac{L_1-L}{L_1-L_\infty}=(1-B)\left\{1-exp\left(-\frac{\pi^2}{4}T_c\right)\right\}+B\{1-exp(-\eta\theta_c)\} \tag{1.28}$$

for constant-pressure expression of filter cakes, and by

$$U_c=\frac{L_1-L}{L_1-L_\infty}$$

$$=(1-B)\left\{1-\sum_{N=1}^{\infty}\frac{8}{(2N-1)^2\pi^2}exp\left(-\frac{(2N-1)^2\pi^2}{4}T_c\right)\right\}$$

$$+B\{1-exp(-\eta\theta_c)\} \tag{1.29}$$

for constant-pressure expression of semisolid materials.[7]

In Eqs. (1.28) and (1.29), U_c is the average consolidation ratio and indicates the degree of deliquoring under a constant pressure. T_c is the consolidation time factor defined by Eq. (1.15). B is an empirical constant defined by

$$B=a_C/(a_E+a_C)=v_{sc\cdot max}/v_{c\cdot max} \tag{1.30}$$

where $v_{sc\cdot max}$ is the maximum liquid volume removed by the secondary consolidation, and $v_{c\cdot max}$ the total liquid volume removed before final equilibrium condition is attained. Fig. 1. 15 illustrates the experimental results of consolidation of filter cakes of Korean kaolin.

Since $C_e(i\pi/2\omega_0)^2\gg\eta$, Eqs. (1.28) and (1.29) become approximately Eq. (1.31) when $\theta_c\gg0$.

$$U_c=\frac{L_1-L}{L_1-L_\infty}\approx1-B\,exp(-\eta\theta_c) \tag{1.31}$$

In consideration of Eq. (1.31), the values of both B and η can be graphically determined from the later stage of the experimental results of $ln(1-U_c)$ vs. θ_c as illustrated in Fig. 1. 16.

It can be seen from Fig. 1. 16 that the B-value of semisolid materials depends upon both the applied pressure p and the initial average void ratio $e_{1\cdot av}$, whereas the η-value is virtually constant. The experimental values of B vs. $p/p_s(e_{1\cdot av})$ are shown in Fig. 1. 17, where $p_s(e_{1\cdot av})$ denotes the solid compressive pressure for

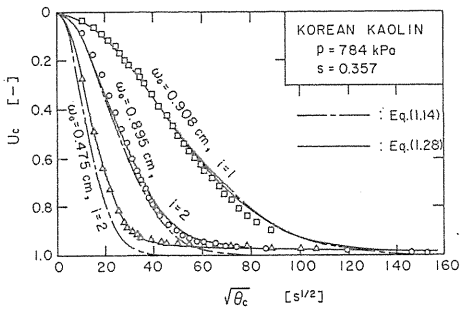

Fig. 1. 15. Constant-pressure expression of Korean kaolin filter cakes. Average consolidation ratio, U_c, vs. $\sqrt{\theta_c}$.

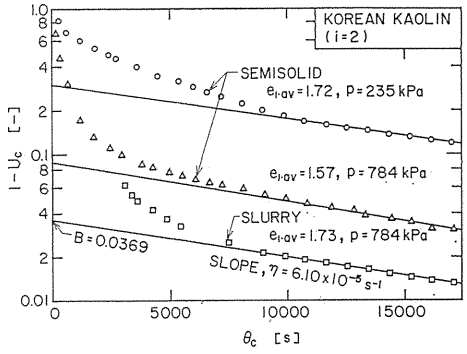

Fig. 1. 16. Determinations of creep constants, B and η.

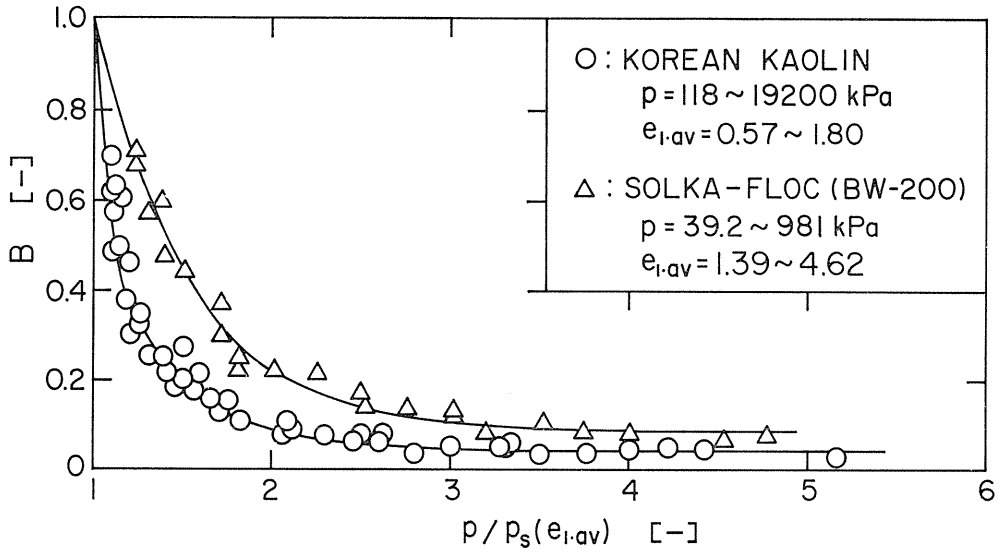

Fig. 1. 17. Creep constant, B, vs. $p/p_s(e_{1\cdot av})$.

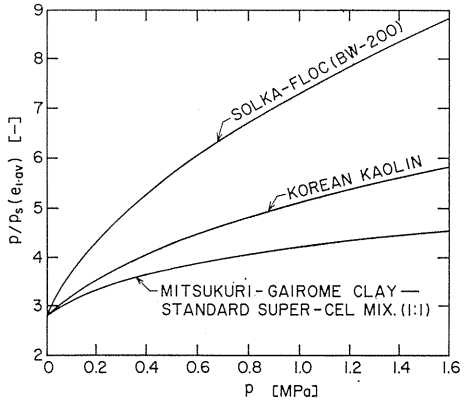

Fig. 1. 18. Theoretical $p/p_s(e_{1\cdot av})$ values of filter cakes.

obtaining final equilibrium void ratio $e_{1\cdot av}$ in compression permeability cell measurements. It is apparent from Fig. 1. 17 that B is substantially constant for $p/p_s(e_{1\cdot av})$-values larger than a limiting value, although it seems that B is a single-valued function of $p/p_s(e_{1\cdot av})$. In Fig. 1. 18, $p/p_s(e_{1\cdot av})$ vs. p for filter cake expression of three materials are shown when expressions are conducted under the same pressure as the filtration pressure. The $p/p_s(e_{1\cdot av})$ values for filter cake expression in industrial practice are larger than about 3 or 4, as may be seen from Fig. 1. 18. Therefore, it can be safely concluded that the values of both B and η are approximately constant for practical expression operations, and they can be viewed as the expression characteristics of the materials themselves.

Modified consolidation coefficient C_e

For determining the experimental C_e-value in Eqs. (1. 28) and (1. 29), a fitting method based on the similarity in shapes of the theoretical U_c-curve and the experimental one can be used. Eq. (1. 28) for filter cake expression can be rearranged as

$$U_{c\cdot corr}=\frac{(L_1-L)-B(L_1-L_\infty)\{1-exp(-\eta\theta_c)\}}{(L_1-L_\infty)(1-B)}$$

$$=1-exp\left(-\frac{\pi^2}{4}T_c\right) \qquad (1.32)$$

and Eq. (1. 29) for semi-solid expression becomes

$$U_{c\cdot corr}=1-\sum_{N=1}^{\infty}\frac{8}{(2N-1)^2\pi^2}exp\left\{-\frac{(2N-1)^2\pi^2}{4}T_c\right\} \qquad (1.33)$$

The experimental values of B, η and the $U_c-\sqrt{\theta_c}$ relation being known, the $U_{c\cdot corr}-\sqrt{\theta_c}$ curve can be pictured from the calculations based upon Eq. (1. 32) or Eq. (1. 33).

In the fitting method for filter cake expression, the time $(\theta_{90})_c$ required for attaining 90% of $U_{c\cdot corr}$ is read in Fig. 1. 19, and C_e is determined by

$$C_e=0.933\omega_0^2/i^2(\theta_{90})_c \qquad (1.34)$$

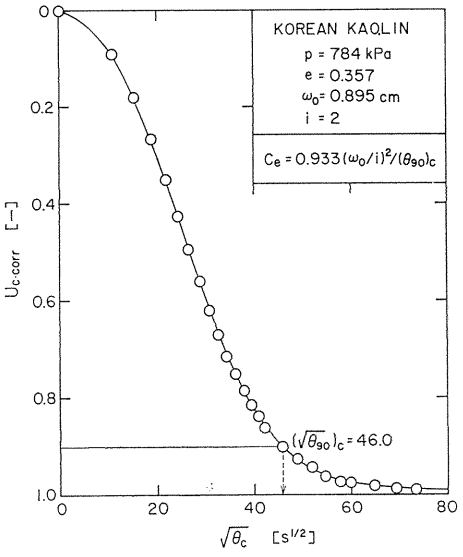

Fig. 1. 19. Fitting method for filter cake consolidation.

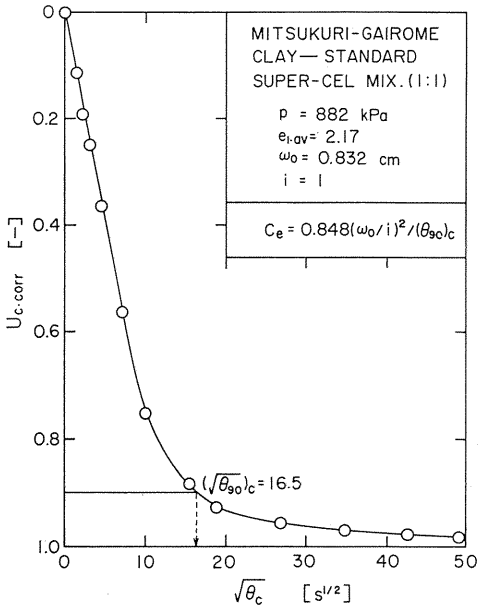

Fig. 1. 20. Fitting method for semisolid consolidation.

In the fitting method for semi-solid expression, the time $(\theta_{90})_c$ is read and C_e can be calculated by Eq. (1. 35) as shown in Fig. 1. 20.

$$C_e=0.848\omega_0^2/i^2(\theta_{90})_c \qquad (1.35)$$

To determine the theoretical C_e-value, eliminating a_E in Eq. (1. 27) by using Eq. (1. 30) and the empirical equations of compression permeability cell data, one can derive the following equation.

$$C_e=\frac{p_{s\cdot av}}{\mu\rho_s C_c(1-B)(\alpha_0+\alpha_1 p_{s\cdot av}{}^n)} \qquad (1.36)$$

where C_c, α_0, α_1, and n are empirical constants for compression permeability cell data, and $p_{s\cdot av}$ denotes the average solid compressive pressure, which is the arith-

metic mean value of the initial average solid compressive pressure $p_s(e_{1\cdot av})$ and the applied expression pressure p. Eq. (1.36) gives a prediction of C_e, and thus the consolidation process can be predicted from calculations based upon compression permeability cell data.

2. Simplified Computation Method

It is apparent that analytical solutions based upon the modified Terzaghi model give somewhat less satisfactory results, especially in the later stages of consolidation. Elaborate solutions based upon the Terzaghi-Voigt combined model coincide very well with experimental data. However, these solutions may not be considered useful mathematical tools in industry, since they include the three empirical constants C_e, B and η, which have to be determined by two graphical plots.

2. 1. Simplified equation for constant-pressure expression of semisolid material

To evaluate the modified consolidation coefficient C_e on the basis of Eq. (1.16) and experimental data, a rather complicated method of curve-fitting has to be employed, since the analytical Eq. (1.16) is not represented by a simple explicit equation but by an infinite series.

It is apparent from Fig. 2. 1 that the U_c vs. $\sqrt{\theta_c}$ relation calculated by Eq. (1.16) is linear and nearly coincides with experimental data in the early stage of constant-pressure consolidation. In the later stage, agreement is poor and the

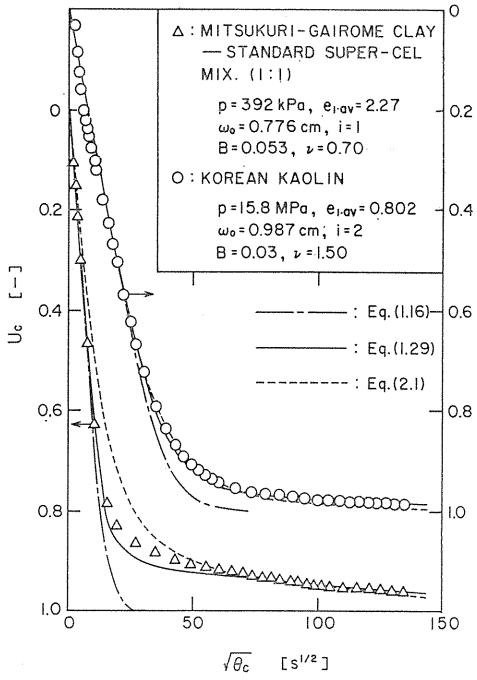

Fig. 2. 1. Constant-pressure expression of semisolid Korean kaolin. U_c vs. $\sqrt{\theta_c}$.

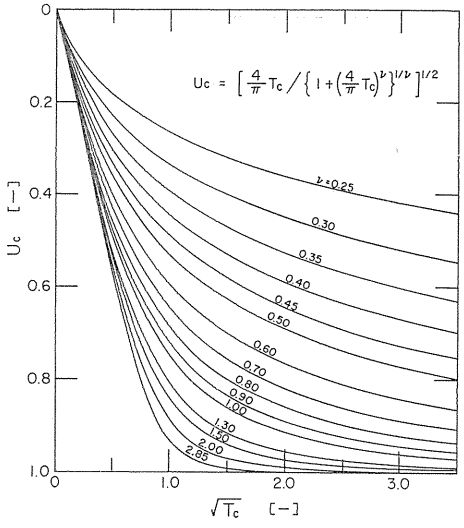

Fig. 2. 2. Average consolidation ratio, U_c vs. $\sqrt{T_c}$ diagram.

calculated curve approaches the final equilibrium ($U_c=1$) more rapidly than the experimental results. Since U_c is directly proportional to $\sqrt{\theta_c}$ for small θ_c values and asymptotically approaches 1 for large θ_c values, one of the simplest equations[8] for use instead of Eq. (1. 16) may tentatively be devised, by reference to Eq. (1. 17), as

$$U_c=\frac{L_1-L}{L_1-L_\infty}=\left[\frac{4}{\pi}T_c\Big/\left\{1+\left(\frac{4}{\pi}T_c\right)^{\nu}\right\}^{1/\nu}\right]^{1/2} \tag{2. 1}$$

In Fig. 2. 2, the average consolidation ratio U_c calculated by Eq. (2. 1) is plotted against the square root of T_c, i. e. $i^2C_e\theta_c/\omega_0{}^2$, for different values of ν. The maximum percentage error in U_c calculated by Eq. (2. 1) with $\nu=2.85$ compared to the theoretical Eq. (1. 16) is only 0. 60. Recently, Sivaram and Swamee[22] presented Eq. (2. 1) with $\nu=2.8$ on purely empirical grounds.

It was previously pointed out that Eq. (1. 16), i. e. Eq. (2. 1) with $\nu=2.85$, gives less satisfactory values. However, it can be seen from Figs. 2. 1 and 2. 2 that Eq. (2. 1) with $\nu<2.85$ may give quite satisfactory values, and the secondary consolidation effect may be taken into account by setting ν as $\nu<2.85$.

In accordance with Eq. (2. 1), experimental values of U_c plotted against $\sqrt{\theta_c}$ yield a straight line in the early stage of constant-pressure consolidation of a semi-solid material, as shown in Fig. 2. 1, and the slope of the line equals $\{4i^2C_e/(\pi\omega_0{}^2)\}^{1/2}$. Thus, the value of C_e being known, rendering the experimental values of $\sqrt{\theta_c}$ in the dimensionless form $\sqrt{T_c}=(i^2C_e\theta_c/\omega_0{}^2)^{1/2}$ enables one to obtain the value of ν by comparing the experimental results of U_c vs. $\sqrt{\theta_c}$ with Fig. 2. 2. Fig. 2. 1 compares the formula of Eq. (2. 1) with experiments, agreement being quite good.

In Fig. 2. 3, experimental values of ν and B are shown. Values of both ν and B are approximately constant for each material; ν can be viewed as a creep charac-

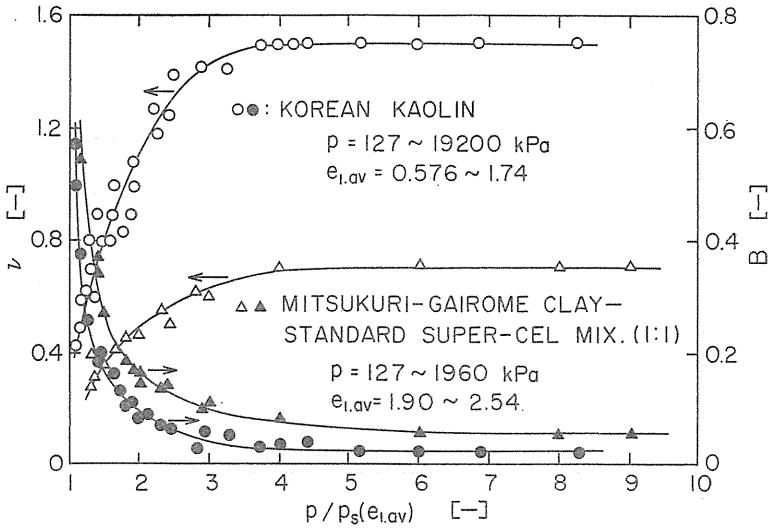

Fig. 2. 3. Consolidation behavior index ν and creep constant B as a function of $p/p_s(e_{1\cdot av})$.

teristic of the materials themselves and may be called the consolidation behavior index.

2. 2. Simplified computation method for constant-pressure expression of filter cakes

The analytical solutions (1. 14) and (1. 28) and the experimental data for constant-pressure expression of filter cakes present inverted S-shape curves of U_c vs. $\sqrt{\theta_c}$, as shown in Fig. 2. 4, whereas the relation for expression of homogeneous semisolid materials is a straight line in the early stage of expression, as shown in Fig. 2. 1. The difference in shape between the two expression curves may be due to the difference in initial voidage distribution in the original materials to be expressed. It has long been known that filter cakes are not uniformly deposited. The cake layer near the filter medium is compact and dry, while the cake surface is wet and soupy. In other words, a portion of the filter cake is already compressed at the beginning of expression. Consequently, the expression rate at an early stage is much lower than that for semisolid materials. As expression proceeds, however, the difference between the two expression curves narrows and is not appreciable at the later stage of expressions of practical importance in industry.

On the basis of the considerations mentioned above, U_c values for expression of filter cakes are calculated by using the simplified Eq. (2. 1) and are illustrated in Fig. 2. 4 by the broken lines. It is apparent from Fig. 2. 4 that the simplified computation method for filter cake expression is fairly accurate at the later stage of $U_c \gtrsim 0.70$.

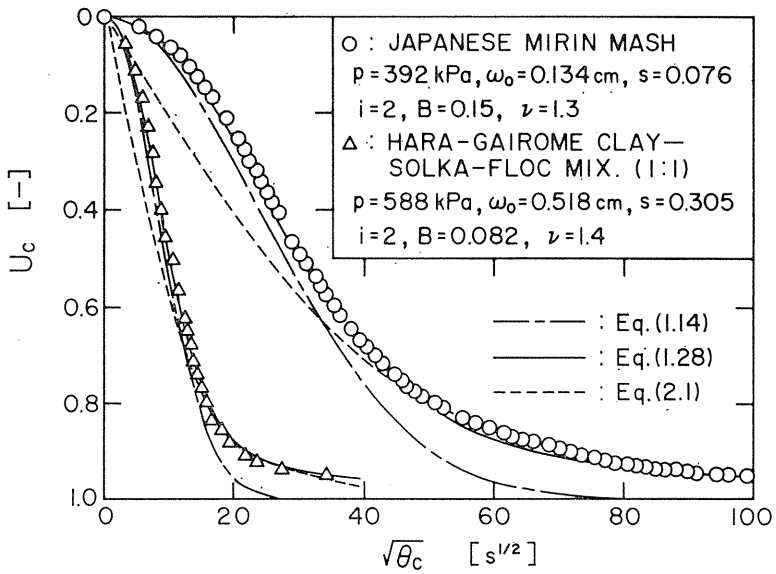

Fig. 2. 4. Constant-pressure expression of filter cakes. U_c vs. $\sqrt{\theta_c}$.

3. Two-Dimensional Expression on Tubular Element

There are many types of expression apparatus used for advanced stages of deliquoring. In an expression-type filter press, the process is one-dimensional expression, with the material being compressed on a plane filter element and the expressed liquid flowing uniaxially, perpendicular to the drainage surface.

In a tube press or a belt press, on the other hand, the material is compressed on a cylindrical filter element and the expressed liquid flows out radially, two-dimensionally, with the rate of expression being quite different from that associated with one-dimensional expression.

In this section, we develop a technique for analyzing the process of two-dimensional expression on a cylindrical filter element.

3. 1. Effective consolidation area factor

Fig. 3. 1 shows the experimental two-dimensional expression apparatus. The central cylindrical filter element is surrounded by an intermediate cylinder which forms the separation chamber, and next to this is an outer cylinder for supplying the compressed air. The circumference of the cylindrical filter element is pierced with a large number of holes and covered with a filter cloth.

Fig. 3. 2 shows the empirical relationship between the consolidation ratio U_c $(=V_c/V_{c\cdot max})$ and the consolidation time $\sqrt{\theta_c}$ of semisolid material, while Fig. 3. 3 shows the empirical relationship between U_c and $\sqrt{T_c}(=\sqrt{C_e\theta_c}/\omega_0)$. V_c is the liquid volume expressed during the time θ_c, $V_{c\cdot max}$ is the total volume of liquid expressed during the compression stage before the equilibrium state of compression is reached, T_c is the consolidation

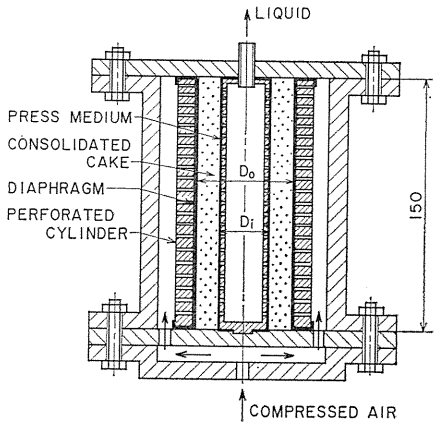

Fig. 3. 1. Experimental apparatus for two-dimensional expression.

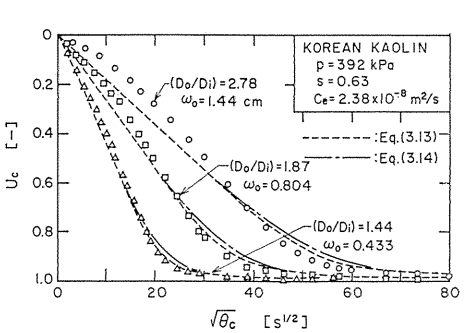

Fig. 3. 2. Average consolidation ratio, U_c vs. $\sqrt{\theta_c}$. (Korean kaolin)

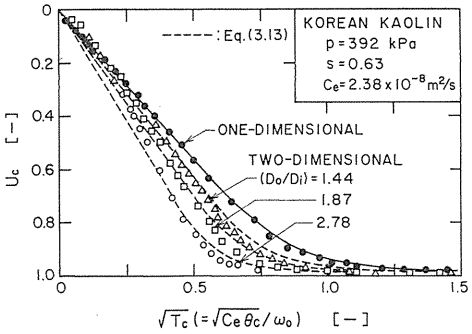

Fig. 3. 3. Average consolidation ratio, U_c vs. $\sqrt{T_c}$.

time factor ($i=1$), and ω_0 is the volume of solids in the original material per unit drainage area. When a material is expressed one-dimensionally, that is, on a plane filter element, the consolidation ratio U_c varies linearly up to $U_c \approx 0.7$, and the consolidation time required to reach a particular consolidation ratio U_c is directly proportional to the solids volume ${\omega_0}^2$. In two-dimensional expression on a cylindrical fliter element, on the other hand, the U_c curve is shaped like a reverse S, as shown, and there is as well some skew in the proportionality between the consolidation time θ_c required to reach a particular value of U_c and the solids volume ${\omega_0}^2$. These differences are more appreciable as the difference increases between the external diameter D_o of the original material and the external diameter D_i of the filter. As Fig. 3. 3 shows, the two-dimensional rate of expression varied quite considerably depending on the value of D_o/D_i. This increase in the two-dimensional rate of expression and the change in the shape of the curve are due to the fact that the effective consolidation area A_e, which is determined by the surface area A_o of the expressed cake and the drainage area $A_m(<A_o)$, is larger than its corresponding value for one-dimensional expression for the same solids volume $\omega_0(A_e=A_o=A_m)$, so that expression occurs more readily in two-dimensional expression operations.

The two-dimensional rate of expression can be expressed approximately in the following way. If the effect of creep is so small as to be negligible, the degree of deliquoring in one-dimensional expression can be expressed by Eq. (1. 16). If Eq. (1. 16) is approximated by the first term of the series, the rate of expression is

$$\left(\frac{dU_c}{d\theta_c}\right)_{\mathrm{I}} = \frac{\pi^2 C_e}{4(W_0/A_m)^2}(1-U_c) \tag{3. 1}$$

where $W_0(=A_m\omega_0)$ is the total solids volume of expressed material. The subscript I signifies one-dimensional expression. If we assume that the two-dimensional rate of expression $(dU_c/d\theta_c)_{\mathrm{II}}$ is controlled by the effective consolidation area A_e and substitute A_e for A_m in Eq. (3. 1), and if we assume that the value of C_e is the same for two-dimensional expression as for one-dimensional expression, the two-dimensional rate of expression can then be expressed in terms of the one-dimensional rate of expression as

$$\left(\frac{dU_c}{d\theta_c}\right)_{\mathrm{II}} = \left(\frac{A_e}{A_m}\right)^2 \frac{\pi^2 C_e}{4(W_0/A_m)^2}(1-U_c) = {j_{\mathrm{II}}}^2\left(\frac{dU_c}{d\theta_c}\right)_{\mathrm{I}} \tag{3. 2}$$

or

$$\left(\frac{dU_c}{dT_c}\right)_{\mathrm{II}} = {j_{\mathrm{II}}}^2\left(\frac{dU_c}{dT_c}\right)_{\mathrm{I}} \tag{3. 3}$$

$j_{\mathrm{II}}(=A_e/A_m)$ is called here the effective consolidation area factor. It is the ratio of the effective consolidation area A_e, taking into account the two-dimensional effect, to the drainage area A_m, and represents the ratio of the rates of expression at any value of U_c, namely $\sqrt{(dU_c/dT_c)_{\mathrm{II}}/(dU_c/dT_c)_{\mathrm{I}}}$.

The effective consolidation area factor j_{II} is determined from consolidation theory in the following way.

Let us assume that, when an expression pressure is acting on a material in a cylindrical filter, all the expressed liquid flows toward the center of the filter and is expressed, with the material all the time maintaining its cylindrical shape, as shown in Fig. 3. 4. When liquid is expressed from the infinitesimal thickness of cake

shown in the figure, the porosity is reduced in proportion. If we now apply the mass balance equation and the equation for the apparent liquid velocity, and for the sake of simplicity use the approximate relationship for one-dimensional expression ($p=p_L+p_s$) as the relationship between the expression pressure p, the hydraulic pressure p_L, and the compression pressure p_s of the solid cake, rather than the general relationship, the consolidation equation will be (assuming negligible creep in the granular structure)

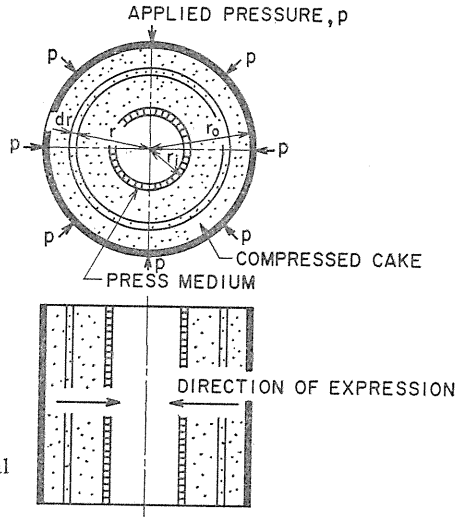

Fig. 3. 4. Compressed cake on cylindrical press medium.

$$\frac{\partial p_L}{\partial \theta_c}=\frac{(1+e)^2}{\mu\rho_s\alpha\left(-\frac{de}{dp_s}\right)}\frac{1}{r}\frac{\partial}{\partial r}\left(r\frac{\partial p_L}{\partial r}\right) \tag{3.4}$$

Solving Eq. (3.4) for constant-pressure expression of a semisolid material with a uniform initial void ratio e_1,[10,23] we obtain the equation for two-dimensional expression

$$U_c=1-\sum_{a_1,a_2,a_3,\cdots}^{\infty}\frac{4U_1^2}{a^2(n_D^2-1)(n_D^2U_0^2-U_1^2)}exp\left\{-\frac{a^2(n_D^2-1)^2}{4}\frac{C_e}{\omega_0^2}\theta_c\right\} \tag{3.5}$$

where

$$U_0=J_0(an_D)Y_0(a)-Y_0(an_D)J_0(a) \tag{3.6}$$

$$U_1=J_1(a)Y_0(a)-J_0(a)Y_1(a) \tag{3.7}$$

$$n_D=D_0/D_i=r_0/r_i \tag{3.8}$$

$$C_e=\frac{1}{\mu\rho_s\alpha\left(-\frac{de}{dp_s}\right)} \tag{1.13}$$

J_0, J_1, Y_0 and Y_1 are Bessel functions of the first and second kind of order 0 and 1, respectively, r_o and r_i are respectively the external and internal radii of the semisolid material at the beginning of consolidation ($\theta_c=0$), and a_1, a_2, a_3, etc., are the first, second, third, etc., roots of the equation,

$$J_1(an_D)Y_0(a)-Y_1(an_D)J_0(a)=0 \tag{3.9}$$

If we approximate Eq. (3.5) by the first term of the series, as was done with Eq. (3.1), the rate of expression will be

$$\left(\frac{dU_c}{d\theta_c}\right)_{\text{II}} = \left\{\frac{a_1(n_D{}^2-1)}{\pi}\right\}^2 \frac{\pi^2 C_e}{4(W_0/A_m)^2}(1-U_c) \tag{3.10}$$

Comparing this equation and Eq. (3.2), we obtain the following expression for the effective consolidation area factor j_{II}:

$$j_{\text{II}} = \frac{a_1(n_D{}^2-1)}{\pi} \approx 0.297 n_D + 0.703 \tag{3.11}$$

The approximation on the right-hand side is used over the range $n_D < 3.0$. Although creep has some effect in an actual expression process, the effect is considered to be about the same for two-dimensional as for one-dimensional expression. For the purpose of determining j_{II} from the ratio of the two expression rates, we can assume that creep has virtually no effect, and that j_{II} values of most actual expression processes can be approximated by Eq. (3.11).

Fig. 3. 5 shows the value of j_{II}, as calculated from the formula, $j_{\text{II}} = \sqrt{(dU_c/dT_c)_{\text{II}}/(dU_c/dT_c)_{\text{I}}}$, by determining the rates of expression for various values of the consolidation time factor T_c from the experimentally determined U_c curve. The results shown were obtained with $U_c \lesssim 0.95$. Near the beginning of consolidation ($T_c \approx 0$), $j_{\text{II}} \approx 1$. As consolidation proceeds, j_{II} increases gradually and then begins to fall, the graph being convex upwards. It is thought that $j_{\text{II}} \to 1$ as $T_c \to \infty$. If $n_D \lesssim 3.0$, as it is in these experiments, the convexity in the curve is extremely slight, and for most of the consolidation stage j_{II} can be taken as being constant. The broken lines in the

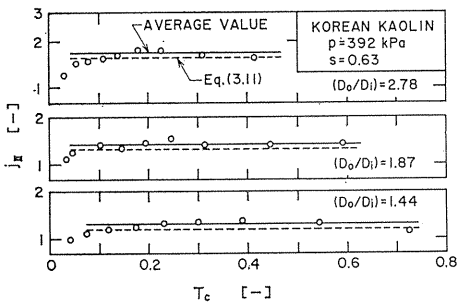

Fig. 3. 5. Effective consolidation area factor, j_{II}, vs. T_c.

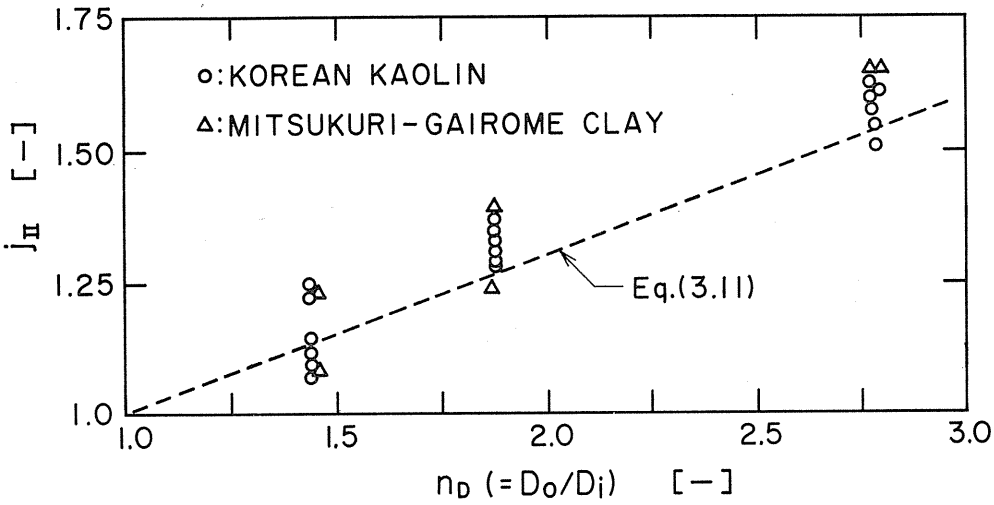

Fig. 3. 6. Effective consolidation area factor, j_{II}, vs (D_0/D_i).

graphs represent the calculated results by Eq. (3. 11), which are very close to the average for the experimental results during the main consolidation period.

Fig. 3. 6 shows a comparison between the average value of j_{II} during the main expression period and the value given by Eq. (3. 11). The experimental values of j_{II} are the average values, which for the sake of convenience were calculated from the mean rate of expression at $U_c=0.9$ rather than using values of dU_c/dT_c in Eq. (3. 3). This graph shows that the average value of j_{II} during the main expression period is independent of the nature or the properties of the material, being determined only by the ratio n_D of the external and internal diameters of the material. In short, this value could be expressed to a good degree of precision by Eq. (3. 11).

3. 2. Computation method for constant-pressure expression

The general expression for the consolidation time required to attain a value U_c is

$$T_c=\int_0^{U_c}\left(\frac{dT_c}{dU_c}\right)dU_c \tag{3.12}$$

If we substitute Eq. (3. 3) into Eq. (3. 12) and treat j_{II} as constant, the time for two-dimensional expression is

$$T_{c\cdot II}=\int_0^{U_c}\frac{1}{j_{II}^{\,2}}\left(\frac{dT_c}{dU_c}\right)_I dU_c=\frac{1}{j_{II}^{\,2}}T_{c\cdot I} \tag{3.13}$$

In other words, if the $U_c-\sqrt{T_c}$ relationship for one-dimensional expression is known, the two-dimensional expression process for the same expression pressure can be estimated from Eq. (3. 13).

Fig. 3. 7 shows that the two-dimensional expression time $\sqrt{T_{c\cdot II}}$ for any value of U_c is point B, or $(1/j_{II})$ times the one-dimensional expression time $\sqrt{T_{c\cdot I}}$ (point C). The solid curves in Fig. 3. 7 represent the results as calculated from Eq. (3. 5). The broken lines in Figs. 3. 2 and 3. 3 represent the estimated results, obtained by calculating j_{II} from Eq. (3. 11) and multiplying by $(1/j_{II})^2$ the time as given by the U_c curve for one-dimensional expression. At the beginning of the consolidation, the difference between estimated and experimental results is greater, the higher the value of D_o/D_i. In most industrial tube presses, however, $D_o/D_i\lesssim 1.5$, so that, for practical purposes, the error of estimation can be disregarded at the beginning of the consolidation stage.

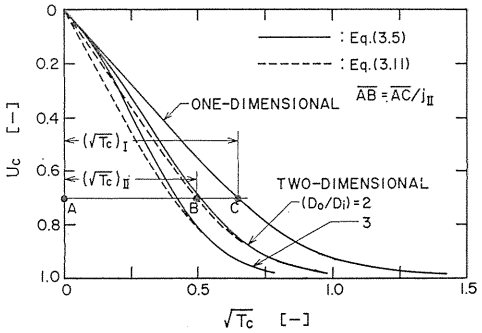

Fig. 3. 7. Prediction of U_c-curve for two-dimensional expression.

If creep is taken into account, the one-dimensional expression of a semisolid material is given fairly accurately by the expression,

$$U_c=\frac{\sqrt{4T_c/\pi}}{\{1+(4T_c/\pi)^{\nu}\}^{1/2\nu}} \tag{2.1}$$

The value of U_c for two-dimensional expression can be determined by substituting Eq. (3.13) into Eq. (2.1), thus:

$$U_c=\frac{\sqrt{4j_{\mathrm{I}}{}^2T_c/\pi}}{\{1+(4j_{\mathrm{I}}{}^2T_c/\pi)^{\nu}\}^{1/2\nu}} \tag{3.14}$$

where ν is the consolidation behavior index, which expresses the effect of creep in the granular structure. The dot-dash line in Fig. 3.2 represents the results as calculated from Eq. (3.14), using the value of ν for one-dimensional expression, and by substituting into the formula, $T_c=C_e\theta_c/\omega_0{}^2$, the value of the consolidation coefficient C_e as obtained by curve fitting of empirical data obtained in one-dimensional consolidation experiments.

4. Constant-Rate Expression of Semisolid Material

In previous chapters, the analysis was limited to constant-pressure expression. Constant-rate and variable-pressure, variable-rate expression operations are more often encountered in industry. However, relatively little work has been reported in connection with constant-rate and variable-pressure, variable-rate expression.[15] This chapter is devoted to extending the previous analytical method for expression under constant pressure to expression under variable pressure. In doing so we shall restrict ourselves here to the constant-rate expression of semisolid material.

4. 1. Estimation of expression pressure

Owing to common engineering practice in constant-rate expression operations, the process may consist of two stages. In the first stage, the deliquoring rate is held constant and the applied pressure p may be increased up to a pre-determined maximum pressure p_{max}; in the second stage, the maximum pressure is maintained until the final equilibrium compression is attained. Fig. 4.1 shows such an expression process. In the figure, q means the rate of deliquoring per unit area (the expression rate) in the constant-rate expression period. In the constant-rate operation, p vs. θ_c is the most important relationship to be estimated.

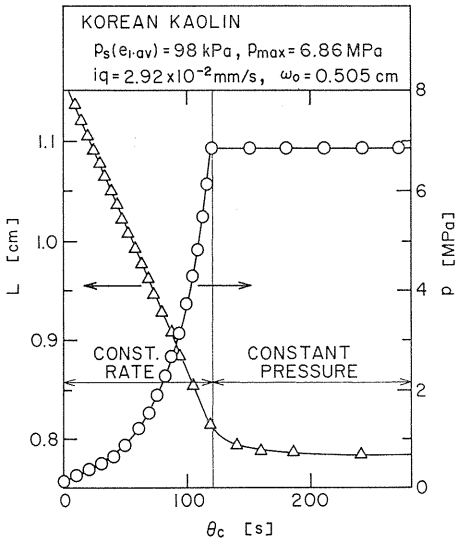

Fig. 4.1. Experimental results under constant-rate expression. Thickness of mixture, L, and expression pressure, p, vs. expression time, θ_c.

For the purpose of determining the relationship between p and θ_c, we introduce the following assumption:[11]

"Internal condition of consolidated cake in the constant-rate operation under the expression pressure p is the same as that in the constant-pressure operation under such a pressure p, when the same volume of liquids is

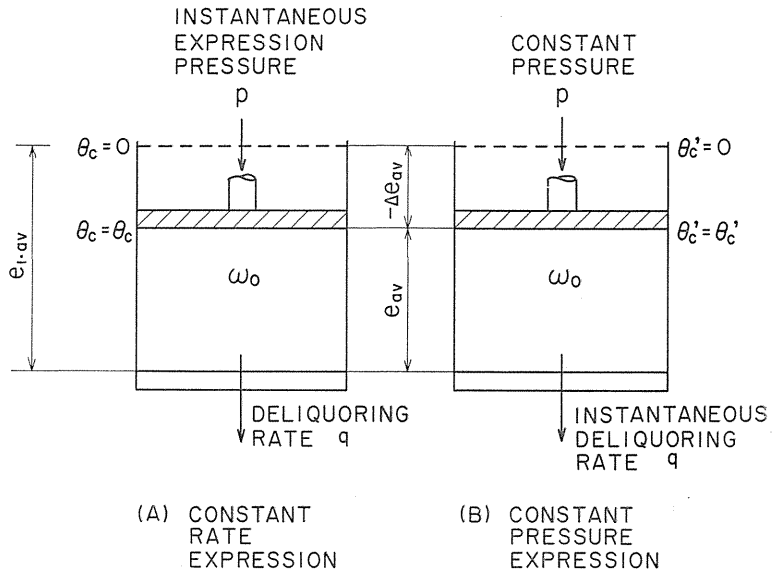

Fig. 4. 2. Comparison between constant-rate and constant-pressure expression processes.

removed from the same amount of the original materials in both operations."

Fig. 4. 2 illustrates both the constant-rate and the constant-pressure operations when the same decreases of average void ratio ($-\Delta e_{av}$) are attained from the same amount of original materials. At this moment, suppose the expression pressure p is the same in both operations. Then, if the above assumption is valid, the instantaneous rates of void reduction ($-de_{av}/d\theta_c$) in the two operations should have the same value.

In the constant-pressure expression operation, remembering $L=\omega_0(1+e_{av})$ and rearranging Eq. (1. 29), the decrease of average void ratio ($-\Delta e_{av}$) is represented by

$$-\Delta e_{av}=-\Delta e_{av\cdot\infty}\left\{(1-B)\left[1-\sum_{N=1}^{\infty}\frac{8}{(2N-1)^2\pi^2}exp\left\{-\frac{(2N-1)^2\pi^2}{4}\frac{i^2C_e\theta_c'}{{\omega_0}^2}\right\}\right]\right.$$

$$\left.+B[1-exp(-\eta\theta_c')]\right\} \qquad (4.1)$$

where θ_c' is the consolidation time, ($-\Delta e_{av\cdot\infty}$) is the total decrease of average void ratio until the final equilibrium compression is attained under the pressure p and can be calculated from the eqation

$$-\Delta e_{av\cdot\infty}=C_c ln p/p_s(e_{1\cdot av}) \qquad (4.2)$$

Differentiating Eq. (4. 1) with respect to θ_c' yields the rate of void reduction ($-de_{av}/d\theta_c'$):

$$-\frac{de_{av}}{d\theta_c'}=-\Delta e_{av\cdot\infty}\left[2(1-B)\frac{i^2C_e}{\omega_0{}^2}\sum_{N=1}^{\infty}exp\left\{-\frac{(2N-1)^2\pi^2}{4}\frac{i^2C_e\theta_c'}{\omega_0{}^2}\right\}\right.$$

$$\left.+B\eta\cdot exp(-\eta\theta_c')\right] \tag{4.3}$$

For constant-rate expression, the following equations are applicable.

$$-\frac{de_{av}}{d\theta_c}=\frac{iq}{\omega_0} \tag{4.4}$$

$$-\Delta e_{av}=\frac{iq}{\omega_0}\theta_c \tag{4.5}$$

If we know the compression data, as shown in Fig. 1. 13, and the relationship between the modified consolidation coefficient C_e and p, as shown in Fig. 4. 3, in advance, we can calculate the pressure change in the constant-rate stage by using Eqs. (4. 1), (4. 3), (4. 4) and (4. 5). If the creep effect of the material is negligible ($B=0$), we can draw Fig. 4. 4, which shows the relationship between p, $(-\Delta e_{av})$ and $(-\omega_0{}^2/i^2\cdot de_{av}/d\theta_c)$, by using Eqs. (4. 1) and (4. 3). In this case, it is easy to obtain the p vs. $(-\Delta e_{av})$ relationship at a given expression rate, as shown in the figure. Then the expression pressure change with time can be calculated from Eq. (4. 5).

Fig. 4. 5 compares the experimental pressure change with the theoretical value based on the above method. The solid line in Fig. 4. 5 represents the calculated result which takes the creep effect into account, while the broken line is based upon the theory in the case of $B=0$. Because of good agreement between theory

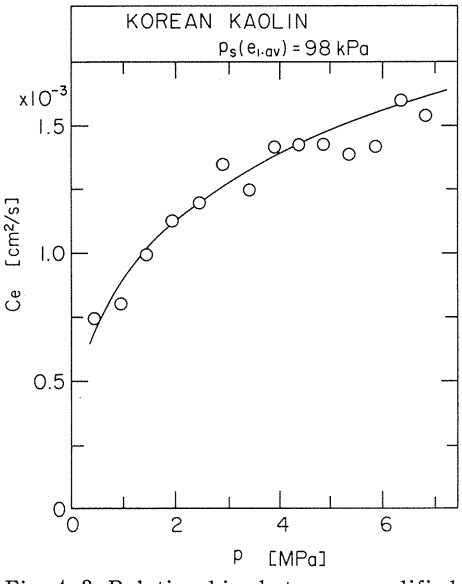

Fig. 4. 3. Relationship between modified consolidation coefficient, C_e, and expression pressure, p.

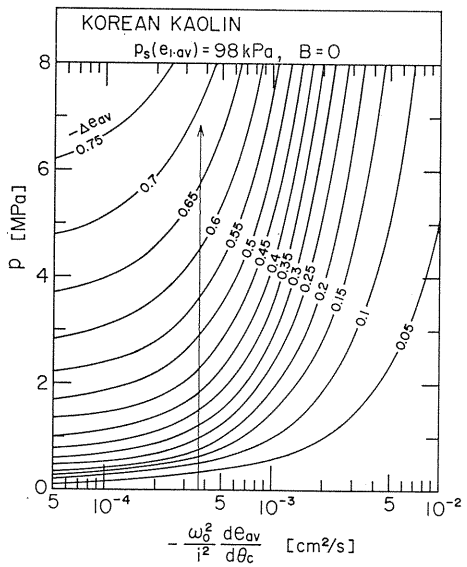

Fig. 4. 4. Graphical determination of p vs. $-\Delta e_{av}$.

and experiment, it is safe to say that the above assumption is acceptable.

4. 2. *Average consolidation ratio*

The average consolidation ratio U_c is defined here in the following form.

$$U_c=\frac{-\Delta e_{av}}{-\Delta e_{av\cdot\infty}(p_{max})} \qquad (4.6)$$

where $(-\Delta e_{av\cdot\infty}(p_{max}))$ is the total decrease of average void ratio under the maximum expression pressure p_{max}. In the constant-rate stage, $(-\Delta e_{av})$ can be calculated from Eq. (4.5). In the constant-pressure stage, we should obtain the time $\theta_{c\cdot1}'$ in Eq. (4.1) at first, which corresponds to $(-\Delta e_{av})$ value when the constant-rate stage is terminated. Now we introduce a new dummy time $\theta_{c\cdot2}'$ which is the sum of $\theta_{c\cdot1}'$ and the time required since the constant-pressure stage began, $\Delta\theta_c$, as follows.

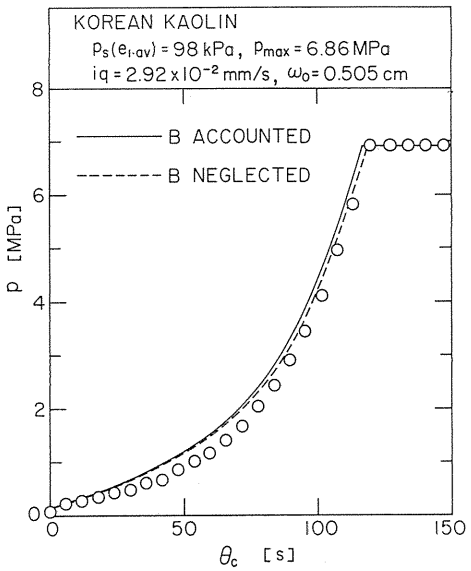

Fig. 4. 5. Comparison of theory and experiment for constant-rate expression.

$$\theta_{c\cdot2}'=\theta_{c\cdot1}'+\Delta\theta_c \qquad (4.7)$$

$(-\Delta e_{av})$ in the constant-pressure stage can be calculated by substituting $\theta_{c\cdot2}'$ into Eq. (4.1).

U_c values are calculated by using Eqs. (4.1), (4.5), (4.6) and (4.7) and are illustrated in Fig. 4. 6.

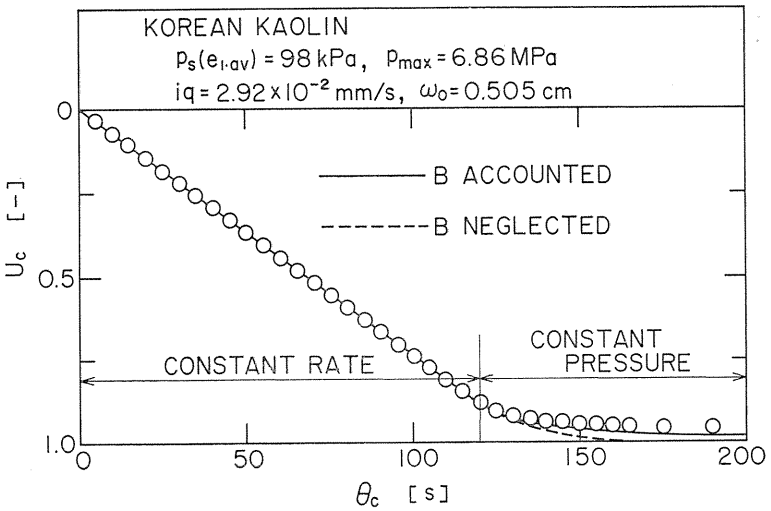

Fig. 4. 6. Average consolidation ratio, U_c, vs. θ_c. (Constant-rate expression)

5. Settling of Thick Slurries due to Consolidation

Sedimentation phenomena occur on a universal scale in both nature and man-directed operations. In spite of the basic importance of these phenomena in widely divergent fields, most previous works were mainly concerned with dispersed suspensions of rather low concentrations, and few quantitative results for flocculated suspensions of high concentrations have been reported. In the higher initial concentration region, solid particles form networks with one another, and a slow subsidence of the interface between the concentrated suspension and clear supernatant occurs. The settling rates in this region may be placed under the control of the internal mechanism of the consolidation or compaction in the suspensions.

The main objectives of this chapter are to present a theoretical and experimental analysis of the settling behavior of fine-particle sediments, which settle by the mechanism of compaction from the beginning of batch sedimentation, and to derive methods of predicting the settling behavior in view of the internal mechanism of consolidation in sediments.[12]

5. 1. Basic equations for settling due to consolidation

In reference to Fig. 5. 1, which shows a differential element in a settling sediment, the driving force for liquid flow through the networks of particles is the hydraulic excess pressure p_L caused by the gravity force of particles lying above the networks.

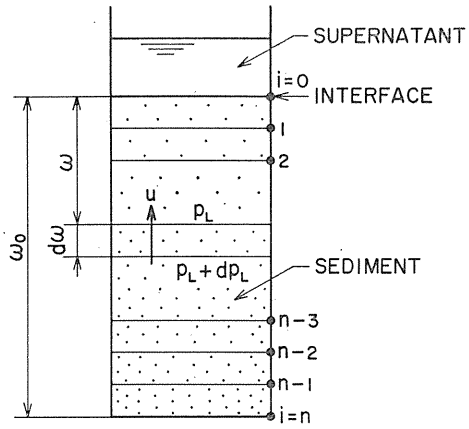

Fig. 5. 1. Schematic diagram of solid volume element in settling sediment.

To derive a basic partial differential equation for hydraulic excess pressure we begin with Darcy's equation (5. 1).

$$u=-K_1\frac{(1-\varepsilon)}{\mu}\frac{\partial p_L}{\partial \omega}=-K_2\frac{\partial p_L}{\partial \omega} \tag{5.1}$$

where u is the local apparent relative velocity of liquid to solids of their differential volume element $d\omega$, ε the local porosity, and K_1 and K_2 the local values of the permeability coefficient and of a modified one, respectively.

The basic differential equation relating the change in u to the time rate of change in local void ratio e can be expressed as

$$\frac{\partial e}{\partial \theta}=-\frac{\partial u}{\partial \omega} \tag{5.2}$$

In Eq. (5. 2), ω is a volume of solids lying above the element as shown in Fig. 5. 1, and the positive signs of ω and u are taken in the same downward direction.

The gravity force of the particles lying above the element is entirely sustained by the hydraulic excess pressure p_L and the solid compressive pressure p_s, provided

side-wall friction between the particles and the container is neglected.

$$p_L+p_s=g(\rho_s-\rho)\omega \tag{5.3}$$

Differentiating Eq. (5.1) with respect to ω gives

$$\frac{\partial u}{\partial \omega}=-K_2\frac{\partial^2 p_L}{\partial \omega^2}-\left(\frac{dK_2}{dp_s}\right)\left(\frac{\partial p_s}{\partial \omega}\right)\left(\frac{\partial p_L}{\partial \omega}\right) \tag{5.4}$$

and substituting the above equation into Eq. (5.2) leads to

$$\frac{\partial e}{\partial \theta}=K_2\frac{\partial^2 p_L}{\partial \omega^2}+\left(\frac{dK_2}{dp_s}\right)\left(\frac{\partial p_s}{\partial \omega}\right)\left(\frac{\partial p_L}{\partial \omega}\right) \tag{5.5}$$

where it is assumed that $K_2=f(p_s)$. On the assumption that the void ratio e is also a function of the solid compressive pressure p_s only, combining Eq. (5.5) with Eq. (5.3) and rearranging yields

$$\frac{\partial p_L}{\partial \theta}=-K_2\left(\frac{dp_s}{de}\right)\left(\frac{\partial^2 p_L}{\partial \omega^2}\right)+\left(\frac{dK_2}{de}\right)\left\{\left(\frac{\partial p_L}{\partial \omega}\right)^2-g(\rho_s-\rho)\left(\frac{\partial p_L}{\partial \omega}\right)\right\} \tag{5.6}$$

Eq. (5.6) can be rewritten by using the following variables;

$$\left.\begin{aligned}
&\phi=p_L/\omega_0(\rho_s-\rho)g \text{ : reduced hydraulic excess pressure}\\
&C_e=-K_2(dp_s/de) \text{ : modified consolidation coefficient}\\
&C_e'=(dK_2/de)\omega_0(\rho_s-\rho)g\\
&C_{eb} : C_e\text{-value for the bottom of sediment } (\omega=\omega_0) \text{ at } T=\infty\\
&z=\omega/\omega_0 \text{ : modified demensionless distance expressed in solids fraction}\\
&T=C_{eb}\theta/\omega_0^2 \text{ : time factor}
\end{aligned}\right\} \tag{5.7}$$

in a dimensionless form as

$$\frac{\partial \phi}{\partial T}=\left(\frac{C_e}{C_{eb}}\right)\frac{\partial^2 \phi}{\partial z^2}+\left(\frac{C_e'}{C_{eb}}\right)\left\{\left(\frac{\partial \phi}{\partial z}\right)^2-\frac{\partial \phi}{\partial z}\right\} \tag{5.8}$$

In solving Eqs. (5.8), the boundary conditions and the initial condition for batch sedimentaiton are

(i) $\phi=0$ at $z=0$

(ii) $\partial\phi/\partial z=0$ at $z=1$

(iii) $\phi=z$ at $T=0$

For numerical treatment, the height of sediments is divided into n parts of equal solids volume. Then the right-hand side of Eq. (5.8) can be transformed to the following Eqs. (5.9), (5.10) and (5.11) by using a finite difference in place of

the derivatives.

Using the boundary condition (i) at $i=0$ (the sediment surface) gives

$$\phi_0=0 \tag{5.9}$$

at $i=1\sim n-1$

$$\left(\frac{d\phi_i}{dT}\right)=n^2\left(\frac{C_{ei}}{C_{eb}}\right)(\phi_{i+1}-2\phi_i+\phi_{i-1})+\left(\frac{C_{ei}'}{C_{eb}}\right)\left\{\frac{n^2}{4}(\phi_{i+1}-\phi_{i-1})^2-\frac{n}{2}(\phi_{i+1}-\phi_{i-1})\right\} \tag{5.10}$$

and using the condition (ii) at $i=n$ (the bottom of sediment) gives

$$\left(\frac{d\phi_n}{dT}\right)=2n^2\left(\frac{C_{en}}{C_{eb}}\right)(\phi_{n-1}-\phi_n) \tag{5.11}$$

where the suffix i denotes the i-th value of the variables from the surface as shown in Fig. 5. 1. The values of the consolidation coefficients C_{ei} and C_{ei}' in Eqs. (5. 10) and (5. 11) depend on the reduced hydraulic excess pressure ϕ_i for a given system and may be determined from the characteristics of the sediments.

The simultaneous differential Eqs. (5. 9), (5. 10) and (5. 11) can be solved by the Runge-Kutta-Gill method by using an electronic computer. To execute the numerical computations, the data of e vs. p_s and K_2 vs. e can be obtained by batch sedimentation tests as described below.

5. 2. Compression and permeability characteristics of sediments

The compression-permeability cell method may generally be worthwhile for analysis of internal flow problems through compressible porous beds under a moderate or relatively high applied pressure.[24] For low compressive pressures of the gravity force of settling sediments, however, it may be safely concluded that the C-P cell method is not adequate for the analysis, because appreciable side friction between the wall of the cell and the compressed cake may lead to substantial errors in the C-P cell data. In addition, the compressed cake under such a low pressure may be too soft for permeability measurements without additional disturbance in the compressed cake. In this chapter, batch sedimentation data are used for determining the compression and permeability characteristics of the sediments.

5. 2. 1. Compression characteristics

Under a given condition of inital concentration of a slurry, the more of the total solids volume ω_0 in a settling container, the higher the sediments H_∞ at the final equilibrium state. The ω_0-H_∞ relation may not be linear because of the difference in degree of compression.

On the assumption that the wall and bottom effects of a container can be neglected, the final porosity ε at a definite depth is a unique value without reference to the total solids volume ω_0 in the container. Then the final porosity ε at the bottom of the container is given by

$$(1-\varepsilon)=d\omega_0/dH_\infty \tag{5.12}$$

On the basis of Eq. (5. 12), the local porosity ε vs. the compressive pressure $p_s(=\omega_0(\rho_s-\rho)g)$ can be determined by graphical or numerical differentiation of the $H_\infty-\omega_0$ curve experimentally obtained.

5. 2. 2. Permeability characteristics

Provided the suspension is homogeneous at time zero, the distribution of the hydraulic excess pressure p_L is linear and the term $(\partial p_L/\partial\omega)_{\theta=0}$ in Eq. (5. 1) equals to $(\rho_s-\rho)g$ throughout the suspension. The modified permeability coefficient K_2 can be calculated by

$$(K_2)_{\theta=0}=v_0/(\rho_s-\rho)g \tag{5. 13}$$

where v_0 is the observed value of the initial settling velocity.

In comparison of Eq. (5. 1) with Kozeny's equation of flow through granular beds, K_2 can be represented by

$$K_2=\varepsilon^3/\{kS_0{}^2(1-\varepsilon)\mu\} \tag{5. 14}$$

where k is Kozeny's constant and S_0 is the effective specific surface area of the flocculated particles. To evaluate the values of $kS_0{}^2$, Eqs. (5. 13) and (5. 14) can be used. As sedimentation progresses, an increase in local compressive pressure p_s may break down the structure of flocs of particles and may result in an increase in $kS_0{}^2$. In this study, however, computations are executed by using Eq. (5. 14) on the assumption of constant $kS_0{}^2$ calculated from the initial settling velocity v_0.

5. 3. Numerical computation procedures

Numerical solutions of the simultaneous differential Eqs. (5. 9), (5. 10) and (5. 11) are obtained by making use of the compression-permeability characteristics determined from settling data as described before. In numerical calculations by the Runge-Kutta-Gill method, the equally spaced volume fraction of solids ($\Delta z=\Delta\omega/\omega_0$) is set to 0. 1, i. e. the number of partition $n=10$, and the interval of time factor (ΔT) is set to 0. 01 or 0. 005 if necessary.

In general, the local compressive pressure p_s at a time T is calculated by Eq. (5. 3) if the hydraulic excess pressure distribution is known. The p_s-distribution being known, the local porosity ε and the local permeability coefficient K_2 at the time T are given by compression-permeability data. The values of C_{ei} and C_{ei}' are determined by Eq. (5. 7) and the value C_{eb} is constant at a given batch sedimentation. Starting from the above-mentioned values at the time T, the distribution of the reduced hydraulic excess pressure ϕ vs. z at the time $T+\Delta T$ is evaluated by using Eqs. (5. 9), (5. 10) and (5. 11).

As a matter of practical computation, starting from the known p_L-distribution

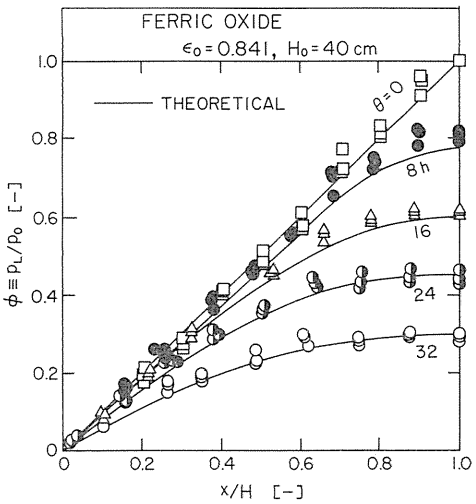

Fig. 5. 2. Hydraulic excess pressure distribution at various times.

at $T=0$, numerical procedures are successively repeated for each time interval. The computed results of the variations of p_L/p_0 vs. x/H, $(1-\varepsilon)$ vs. ω/ω_0, and C_e/C_{eb} vs. ω/ω_0 are illustrated in Fig. 5. 2, Fig. 5. 3 and Fig. 5. 4, respectively, where

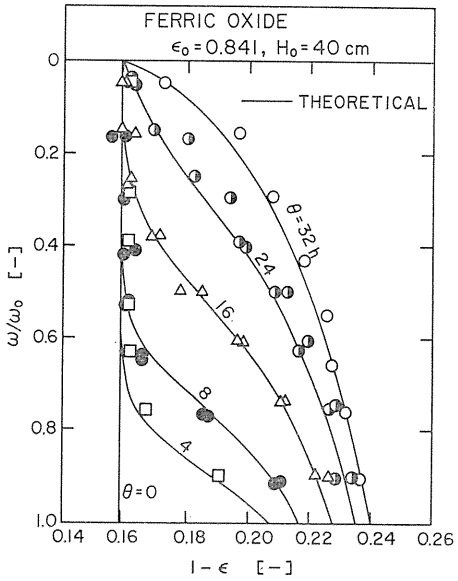

Fig. 5. 3. Concentration distribution at various times.

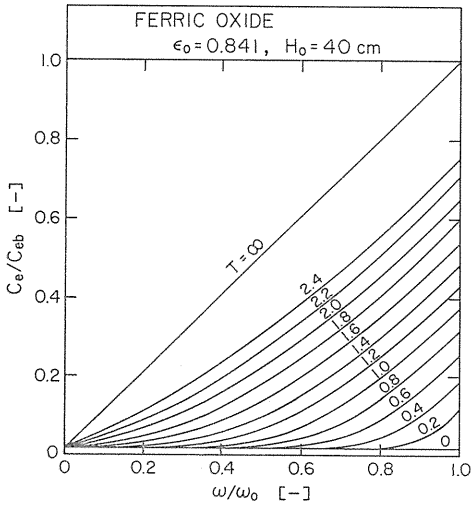

Fig. 5. 4. Distribution of consolidation coefficient at various time factors.

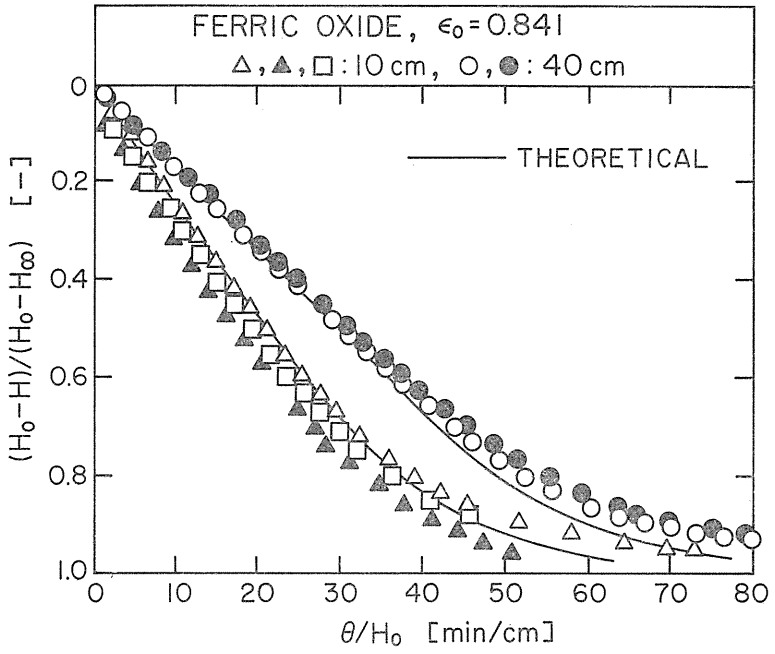

Fig. 5. 5. Consolidation ratio $(H_0-H)/(H_0-H_\infty)$ vs. θ/H_0.

p_0 is the maximum hydraulic excess pressure at the bottom at $\theta_c=0$, x the distance measured from the surface of settling sediments, H the height of settling sediment, H_0 the initial height of suspension and ε_0 the initial porosity of suspension. It can be seen from the figures that a reasonable coincidence between theories and experiments is attained.

The change in porosity distribution with time being known, the settling curve (the degree of consolidation vs. time) can be determined as illustrated in Fig. 5. 5. In the figure, the observed results $(H_0-H)/(H_0-H_\infty)$ vs. θ/H_0 are also plotted. In later periods of settling, the calculated lines tend to approach the final equilibrium, i. e. $(H_0-H)/(H_0-H_\infty)=1$, faster than the observed results. This may be primarily due to the presumption of constant kS_0^2, which may vary more or less during actual settling operations.

6. Principles of Hydraulic Expression

Filter presses are used widely in the chemical and food industries, in sewage sludge treatment and in other applications. In the operation of a conventional filter press, the pattern of filtrate flow changes after the filter chambers of the press are completely filled with filter cake. This change in pattern necessarily causes a change in the hydraulic pressure and compressive pressure distributions through the filter cake, leading to a reduction in the moisture content of filter cakes. This phenomenon is called here filtration-consolidation.

In this chapter, filtration-consolidation in filter press operation is discussed by using a two-dimensional consolidation equation.

6. 1. Mechanism of filter press deliquoring

In Fig. 6. 1, idealized operation of a filter press is shown. In the normal

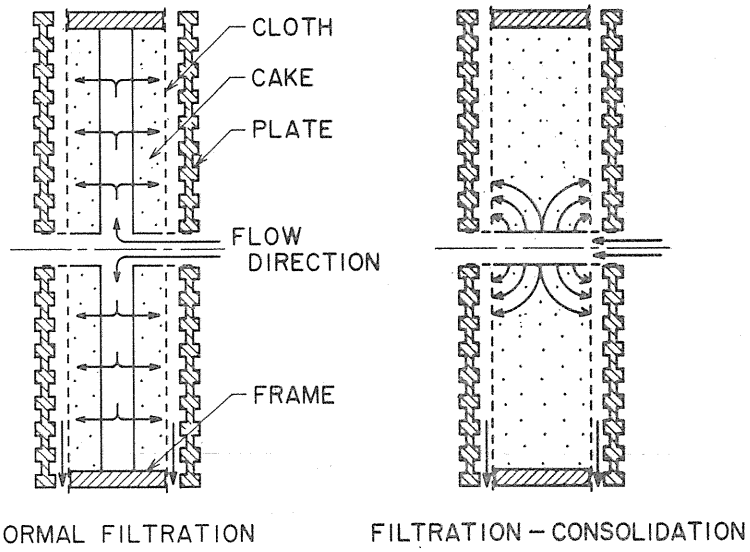

Fig. 6. 1. Flow patterns of filtrate in plate-and-frame press.

filtration period, the surface of the filter cake becomes parallel to the filter medium, and the direction of filtrate flow is perpendicular to the filter medium as illustrated at the left in Fig. 6. 1. When the press becomes "full" of filter cakes, the filtrate will flow only through the portion of the cake near the feed inlet as illustrated at the right in Fig. 6. 1. The solid compressive pressure p_s in cake is produced by the frictional drag of filtrate as it traverses the cake solids. The porosity distribution in a filter cake varies from a maximum at the unconsolidated cake surface to its minimum at the medium, where the p_s-value is maximum and equals the pressure drop across the cake. When the filtrate flow pattern through the filter cake is changed, a new p_s-distribution will develop in the cake, resulting in substantial decrease of local porosities. The filter cake is thus changed from its initial form, which may be termed normal.

In dealing with the mathematics of this deliquoring process, the operation should be divided into two parts, because different flow mechanisms occur in each part. In the first part, the flow mechanism is actually filtration; in the second part, the mechanism is filtration-consolidation.

6. 2. Filtration period

In the filtration period, Ruth's filtration equation in the form

$$\frac{dv_f}{d\theta_f}=\frac{K}{2}\frac{1}{v_f+v_m} \tag{6.1}$$

$$K=\frac{2p(1-ms)}{\mu\rho s\alpha_{av}} \tag{6.2}$$

is applicable. By means of a mass balance, it is possible to calculate the maximum filtrate volume $v_{f.max}$ in the filtration period in accord with Eq. (6. 3).

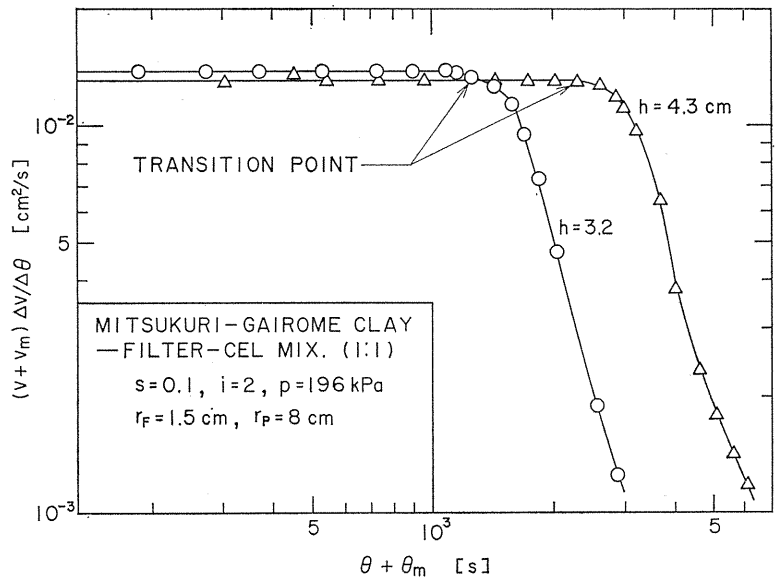

Fig. 6. 2. Determination of transition point between filtration and filtration-consolidation periods.

$$v_{f\cdot max}=\frac{h\rho_s(1-ms)(1-\varepsilon_{av})}{2\rho s} \tag{6.3}$$

In Eq. (6.3), h represents the thickness of the filter chamber, and ε_{av} the average porosity of the cake. The end of the normal filtration period can also be easily determined by an experimental method, as illustrated in Fig. 6. 2. It is apparent from both theoretical and experimental points of view that $(v+v_m)\cdot(\Delta v/\Delta\theta)$ is constant for constant-pressure filtration if Ruth's filtration equation holds true, where v is liquid volume removed per unit area of filter medium, θ the deliquoring time and θ_m the fictitious filtration time accounting for medium resistance.

6. 3. Filtration-consolidation period

The filtration period ends when the filter chamber is "full" of a normal filter cake, and further deliquoring proceeds on the principle of filtration-consolidation. We use a cylindrical coordinate to represent a circular filter press of center-feed type, as illustrated in Fig. 6. 3.

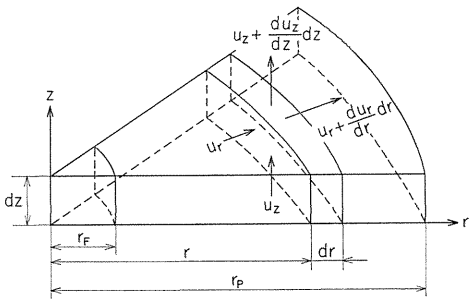

Fig. 6. 3. Cylindrical coordinate system to represent filter chamber.

The apparent velocity of liquid in the r direction, u_r, can be represented by

$$u_r=-\frac{(1+e)}{\mu\rho_s\alpha}\frac{\partial p_L}{\partial r} \tag{6.4}$$

In the z direction,

$$u_z=-\frac{(1+e)}{\mu\rho_s\alpha}\frac{\partial p_L}{\partial z} \tag{6.5}$$

where e is the local value of void ratio, and α the local specific resistance of filter cake. The mass balance of liquid in an infinitesimal layer of cake leads to the continuity equation in the form

$$\frac{\partial e}{\partial\theta_c}=-(1+e)\left(\frac{\partial u_r}{\partial r}+\frac{u_r}{r}+\frac{\partial u_z}{\partial z}\right) \tag{6.6}$$

where θ_c is the filtration-consolidation time. To simplify the equation, we use the relation between the solid compressive pressure p_s and the hydraulic pressure p_L given by the following equation:

$$p_s=p-p_L \tag{6.7}$$

The coefficient of volume change m_v of the infinitesimal layer under consolidation is defined by Eq. (6.8) in soil mechanics.

$$m_v=-\frac{1}{1+e}\frac{de}{dp_s} \tag{6.8}$$

If Terzaghi's coefficient of consolidation C_v defined by

$$C_v=\frac{(1+e)}{\mu\rho_s m_v\alpha} \tag{6.9}$$

can be assumed to be constant, substituting Eqs. (6.4), (6.5), (6.7) and (6.8) into Eq. (6.6) yields the consolidation equation

$$\frac{\partial p_L}{\partial\theta_c}=C_v\left(\frac{\partial^2 p_L}{\partial r^2}+\frac{1}{r}\frac{\partial p_L}{\partial r}+\frac{\partial^2 p_L}{\partial z^2}\right) \tag{6.10}$$

For solving Eq. (6.10) under a constant applied pressure p, the following initial and boundary conditions can be used for filter cakes of moderate compressibility.

$$\text{I. C.}: p_L=p\cdot sin(\pi iz/2h) \tag{6.11}$$

$$\text{B. C.}: p_L=0 \quad \text{at} \quad z=0 \tag{6.12}$$

$$\text{B. C.}: \partial p_L/\partial z=0 \quad \text{at} \quad z=h/i \tag{6.13}$$

$$\text{B. C.}: p_L=p \quad \text{at} \quad r=r_F \tag{6.14}$$

$$\text{B. C.}: \partial p_L/\partial r=0 \quad \text{at} \quad r=r_P \tag{6.15}$$

where i is the number of drainage surfaces, r_F the radius of channel for carrying slurry, and r_P the radius of filter chamber.

The solution of Eq. (6.10) for filter cakes of moderate compressibility is given by[13,14]

$$p_L=2p\sum_{N=1}^{\infty}sin\left\{\frac{(2N-1)\pi}{2}\frac{iz}{h}\right\}\left\{\frac{2E_N}{(2N-1)\pi}\right.$$
$$\left.+\sum_{M=1}^{\infty}\frac{\pi^2\psi_M{}^2}{4}C_{NM}exp\left[-\left\{\psi_M{}^2+\frac{(2N-1)^2\pi^2}{4}\frac{i^2}{h^2}\right\}C_v\theta_c\right]U_{0M}\right\} \tag{6.16}$$

where

$$E_N=\left[I_0\left\{\frac{(2N-1)\pi ir}{2h}\right\}K_1\left\{\frac{(2N-1)\pi ir_P}{2h}\right\}+I_1\left\{\frac{(2N-1)\pi ir_P}{2h}\right\}\right.$$
$$\left.\times K_0\left\{\frac{(2N-1)\pi ir}{2h}\right\}\right]\Big/\left[I_0\left\{\frac{(2N-1)\pi ir_F}{2h}\right\}K_1\left\{\frac{(2N-1)\pi ir_P}{2h}\right\}\right.$$
$$\left.+I_1\left\{\frac{(2N-1)\pi ir_P}{2h}\right\}K_0\left\{\frac{(2N-1)\pi ir_F}{2h}\right\}\right] \tag{6.17}$$

$$C_{NM}=\frac{Y_0{}^2(\psi_M r_F)Y_1{}^2(\psi_M r_P)}{Y_0{}^2(\psi_M r_P)-Y_1{}^2(\psi_M r_P)}\int_{r_F}^{r_P}\left\{\delta_{1N}-\frac{4E_N}{(2N-1)\pi}\right\}rU_{0M}dr \tag{6.18}$$

$$U_{0M}=\{J_0(\psi_M r)Y_1(\psi_M r_P)-J_1(\psi_M r_P)Y_0(\psi_M r)\}/Y_1(\psi_M r_P) \tag{6.19}$$

δ_{1N} is Kronecker's δ, which is equal to 1 for $N=1$ and to zero for $N\neq 1$. J and Y are Bessel functions of the first and second kinds, respectively. I and K are modified Bessel functions of the first and second kinds, respectively. The subscripts are the order of the Bessel function. The ψ_M are the positive roots of the equation

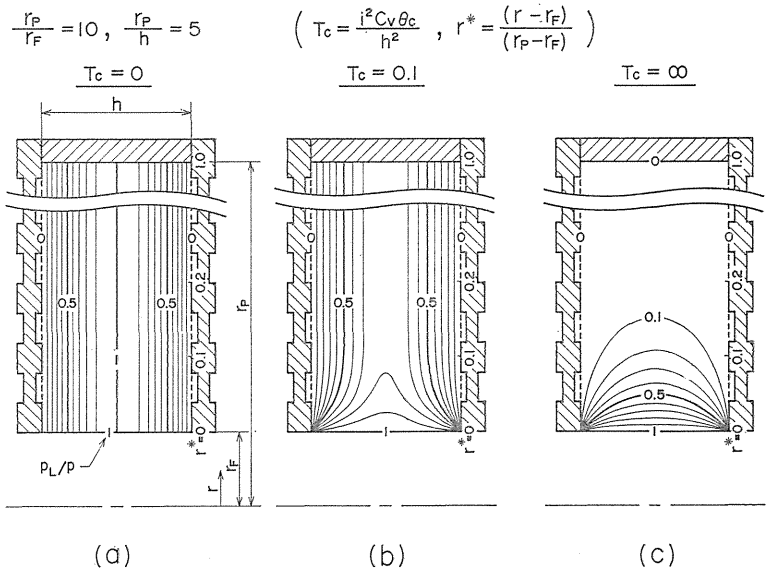

Fig. 6. 4. Change of hydraulic pressure p_L-distribution with time in filter press.

$$J_0(\psi r_F)Y_1(\psi r_P)-J_1(\psi r_P)Y_0(\psi r_F)=0 \tag{6.20}$$

The hydraulic pressure distributions in the circular filter press of center-feed type are calculated by using Eq. (6. 16), and the results are shown in Fig. 6. 4 in a dimensionless form of p_L/p for $i=2$. In Fig. 6. 4, T_c is the dimensionless time factor defined by $T_c=i^2C_v\theta_c/h^2$, and r^* is the dimensionless radius defined by $r^*=(r-r_F)/(r_P-r_F)$. Fig. 6. 4 (a) shows the beginning of filtration-consolidation when $T_c=0$. Fig. 6. 4 (b) represents the condition of about 20% consolidation compared with the final equilibrium filtration-consolidation, which is shown in Fig. 6. 4 (c). It is apparent from the figure that at the end of the filtration-consolidation stage the hydraulic pressure is nearly equal to zero throughout most of the filter cake. Therefore, the average porosity of the filter cake should be nearly equal to that of the compressed cake under the expression pressure which is equal to the final filtration pressure. In practical filter press operation, however, movement of cake solids in filter chambers is considerably retarded by the friction between cake solids and filter medium. Thus, such a marked deliquoring due to filtration-consolidation is not expected in practice.

The filtration velocity in the filtration-consolidation stage is represented by

$$q_c=\frac{1}{\pi({r_P}^2-{r_F}^2)}\int_{r_F}^{r_P}2\pi r|u_{z=0}|dr \tag{6.21}$$

where $u_{z=0}$ means the apparent velocity of liquid at the filter medium. If we designate the filtration velocity at the beginning and end of the filtration-consolidation stage by q_{c0} and $q_{c\infty}$, respectively, a measure of the extent of filtration-consolidation is given by the average consolidation ratio U_c for Eq. (6. 22):

$$U_c=\frac{q_{c0}-q_c}{q_{c0}-q_{c\infty}}$$

$$=\left[\sum_{N=1}^{\infty}\sum_{M=1}^{\infty}\frac{(2N-1)\psi_M C_{NM}}{Y_1(\psi_M r_P)}\{Y_1(\psi_M r_F)J_1(\psi_M r_P)-Y_1(\psi_M r_P)J_1(\psi_M r_F)\}\right.$$

$$\left.\times\left(1-exp\left[-\left\{\psi_M{}^2+\frac{(2N-1)^2\pi^2}{4}\frac{i^2}{h^2}\right\}C_v\theta_c\right]\right)\right]\Big/$$

$$\left[\sum_{N=1}^{\infty}\sum_{M=1}^{\infty}\frac{(2N-1)\psi_M C_{NM}}{Y_1(\psi_M r_P)}\{Y_1(\psi_M r_F)J_1(\psi_M r_P)-Y_1(\psi_M r_P)\ J_1(\psi_M r_F)\}\right] \tag{6.22}$$

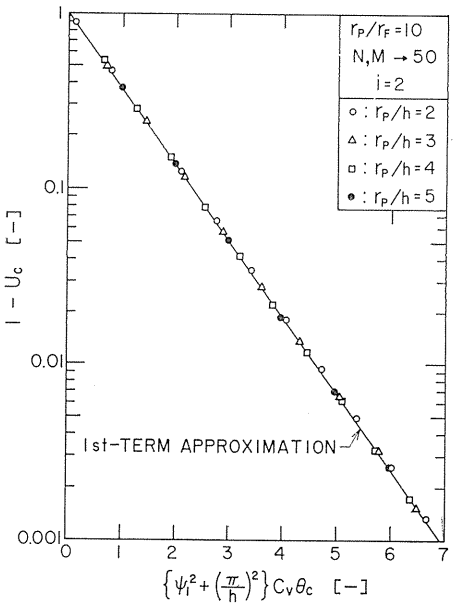

Fig. 6. 5. Comparison between Eq. (6.22) and its 1st-term approximation.

Eq. (6.22) has a rather complicated form. As shown in Fig. 6.5, however, even without such tedious calculation we can use a convenient first term approximation of Eq. (6.22), in the following form.

$$U_c=1-exp\left\{-\left(\psi_1{}^2+\frac{\pi^2}{4}\frac{i^2}{h^2}\right)C_v\theta_c\right\} \tag{6.23}$$

Fig. 6. 6. compares the experimental data for filtration-consolidation of a mixture of Mitsukuri-Gairome clay and Filter-cel with calculations based upon Eq. (6.23). Disagreement between the experimental data and the calculations may be due to the fact that the movement of cake solids is retarded by friction between cake solids and filter medium.

In a practical filter press, $\psi_1{}^2 \ll \pi^2 i^2/(4h^2)$ and Eq. (6.23) coincides with the equation of average consolidation ratio of Terzaghi's model for one-dimensional filter cake consolidation.[25]

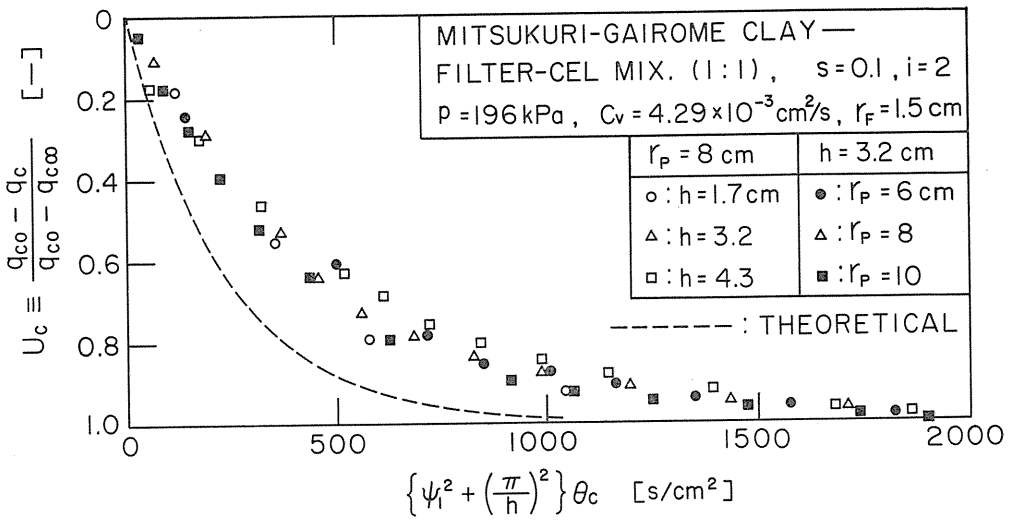

Fig. 6. 6. Comparison of theory and experiment for a conventional filter press.

Conclusions

Analytical solutions and a semi-theoretical equation for batchwise expression, settling of thick slurry and hydraulic expression are presented, and their industrial applications are summarized.

1) The mechanism of both filter cake and semisolid expression consists of two parts: primary consolidation and the secondary consolidation due to creep effect. The expression process can be well analyzed by combining Terzaghi's and Voigt's models.

2) The time for attaining a specified value of the degree of expression is proportional to ω_0^2 and is inversely proportional to i^2. Analytical determination of the original thickness of the material plays an important role in equipment design.

3) On the basis of the analytical solution of Terzaghi's model, a simplified semitheoretical equation is derived. This can be successfully applied to constant-pressure expression, not only of semisolid materials but also of filter cakes.

4) Two-dimensional expression on tubular element can be analyzed well by using the concept of effective consolidation area factor.

5) Constant-rate expression can be treated as a continuous succession of constant-pressure expressions and can be analyzed well by using the analytical solution of the constant-pressure process.

6) The settling of thick slurries can be well analyzed in view of the internal consolidation mechanism. Compression-permeability characteristics in the low-pressure region can be well obtained by batch sedimentation tests.

7) Hydraulic deliquoring occurs after the filtrate flow pattern in a conventional filter press changes from linear to the non-unidimensional. An analytical method for filtration-consolidation phenomena is presented.

Acknowledgments

The authors wish to thank the Ministry of Education of Japan (Special Research Project on Environmental Science, Grants No. 503043, 56030043, 57030039, 58030038 and 59030046 and Scientific Research Project (A), Grant No. 57430022) for its support of most of the work presented here. They also wish to express their sincere gratitude to the Asahi Glass Foundation for Contribution to Industrial Technology for supporting work leading to the publication of this article.

Nomenclature

A_e = effective consolidation area [m^2]
A_m = drainage area of press medium [m^2]
A_o = surface area of original semi-solid material [m^2]
a_C = coefficient of compressibility due to secondary consolidation defined by $a_C=(1+e)/E_2$ [Pa^{-1}]
a_E = coefficient of compressibility due to primary consolidation defined by $a_E=(1+e)/E_1$ [Pa^{-1}]
B = creep constant representing the ratio of consolidation by the so-called secondary consolidation to the total consolidation [−]
C_c = empirical constant for compression data [−]
C_e = modified consolidation coefficient [m^2/s]
C_v = Terzaghi's consolidation coefficient [m^2/s]
D_i = diameter of cylindrical press medium [m]
D_o = diameter of original semisolid material [m]
E_1 = elastic coefficient of Terzaghi element [Pa]
E_2 = elastic coefficient of Voigt element [Pa]
e = local void ratio [−]
e_0 = empirical constant for compression data [−]
$e_{1\cdot av}$ = initial average void ratio [−]
G = viscosity of Voigt element [Pa·s]
g = acceleration of gravity [m/s^2]
H = height of settling sediment at time θ [m]
H_0 = initial height of suspension, i. e. H at $\theta=0$ [m]
H_∞ = final equilibrium value of H, i. e. H at $\theta=\infty$ [m]
h = chamber thickness of filter press [m]
I_ν = modified Bessel function of the first kind of order ν [−]
i = number of drainage surfaces [−]
J_ν = Bessel function of the first kind of order ν [−]
j_{II} = effective consolidation area factor [−]
K = Ruth's filtration coefficient defined by $K=\dfrac{2p(1-ms)}{\mu\rho s\alpha_{av}}$ [m^2/s]
K_w = modified filtration coefficient [m^2/s]
K_ν = modified Bessel function of the second kind of order ν [−]
K_1 = Darcy's permeability coefficient [m^2]
K_2 = modified permeability coefficient defined by Eq. (5.1) [m^2/Pa·s]

L = thickness of solid-liquid mixture [m]
L_0 = initial thickness of the mixture [m]
L_1 = thickness of mixture at the end of filtration period, i. e. at the beginning ($\theta_c=0$) of consolidation period [m]
L_∞ = final thickness of compressed cake at $\theta_c=\infty$ [m]
L_m = fictitious (L_0-L) value equivalent to medium resistance [m]
m = ratio of wet to dry cake mass [−]
m_v = coefficient of volume change defined by $m_v=-\frac{1}{1+e}\frac{de}{dp_s}$ [Pa^{-1}]
n = compressibility coefficient of cake [−]
n_D = ratio of outer to inner diameter of original material [−]
p = applied pressure [Pa]
p_L = local hydraulic pressure or hydraulic excess pressure [Pa]
p_s = local solid compressive pressure [Pa]
$p_{s\cdot 1}$ = local solid compressive pressure of material at beginning of consolidation [Pa]
$p_{s\cdot av}$ = average p_s-value of cake during consolidation process [Pa]
$p_s(e_{1\cdot av})$ = solid compressive pressure where final equilibrium void ratio $e_{1\cdot av}$ is attained [Pa]
p_0 = maximum liquid pressure at the bottom of sediments at $\theta=0$ [Pa]
q = rate of deliquoring per unit area [m/s]
r = radial coordinate of the three-dimensional system of cylindrical coordinates [m]
r_F = radius of channel for carrying slurry [m]
r_i = radius of cylindrical press medium [m]
r_o = radius of original semisolid material [m]
r_P = radius of filter chamber [m]
s = mass fraction of solid in original mixture [−]
T_c = time factor of consolidation [−]
T_f = time factor of filtration [−]
T_m = time factor accounting for medium resistance [−]
U_c = average consolidation ratio [−]
$U_{c\cdot corr}$ = average consolidation ratio defined by Eqs. (1. 32) and (1. 33) [−]
U_f = filtration ratio [−]
U_m = filtration ratio accounting for medium resistance [−]
u = local value of apparent relative velocity of liquid to solid [m/s]
u_r = apparent velocity of liquid in the r direction [m/s]
u_z = apparent velocity of liquid in the z direction [m/s]
v = liquid volume removed per unit area of filter medium [m]
$v_{c\cdot max}$ = total liquid volume removed before final equilibrium condition [m]
v_f = filtrate volume per unit area of filter medium [m]
v_m = fictitious filtrate volume accounting for medium resistance [m]
v_0 = initial settling velocity of surface of suspensions [m/s]
Y_ν = Bessel function of the second kind of order ν [−]
z = axial coordinate of the three-dimensional system of cylindrical coordinates [m]
α = local specific resistance of filter cake [m/kg]
α_{av} = average value of α [m/kg]
α_0 = empirical constant for compression permeability cell data [m/kg]

α_1 = empirical constant for compression permeability cell data [m/(kg·Pa^n)]
ε = local porosity [−]
η = creep constant defined by $\eta = E_2/G$ [s^{-1}]
θ = deliquoring time [s]
θ_c = consolidation time [s]
θ_m = fictitious filtration time [s]
θ_{90} = consolidation time required for attaining 90% of U_c [s]
μ = viscosity of liquid [Pa·s]
ν = consolidation behavior index [−]
ρ = density of liquid [kg/m^3]
ρ_s = true density of solid [kg/m^3]
ω = variable for indicating an arbitrary position in cake, i. e. volume of solid per unit sectional area [m]
ω_0 = total solid volume in cake per unit sectional area [m]

References

1) C. F. Gurnham and H. J. Masson, "Expression of Liquids from Fibrous Materials", Ind. End. Chem., **38**, 1309 (1946).
2) E. C. Koo, "Expression of Vegetable Oils", Ind. Eng. Chem., **34**, 342 (1942).
3) H. Taguchi and S. Nagai, "Filtration and Expession in Fermentation Industries", J. Chem. Soc. Japan, Ind. Chem. Sec., **67**, 708 (1964).
4) I. Körmendy, "A Pressing Theory with Validating Experiments on Apples", J. Food Science, **29**, 631 (1964).
5) M. Shirato, T. Murase, H. Kato and S. Fukaya, "Studies on Expression of Slurries under Constant Pressure", Kagaku Kōgaku, **31**, 1125 (1967).
6) M. Shirato, T. Murase, H. Kato and S. Fukaya, "Fundamental Analysis for Expression under Constant Pressure", Filtration & Separation, **7**, 277 (1970).
7) M. Shirato, T. Murase, A. Tokunaga and O. Yamada, "Calculations of Consolidation Period in Expression Operation", J. Chem. Eng. Japan, **7**, 229 (1974).
8) M. Shirato, T. Murase, K. Atsumi, T. Aragaki and T. Noguchi, "Industrial Expression Equation for Semi-Solid Materials of Solid-Liquid Mixture under Constant Pressure", J. Chem. Eng. Japan, **12**, 51 (1979).
9) M. Shirato, T. Murase and K. Atsumi, "Simplified Computational Method for Constant Pressure Expression of Filter Cakes", J. Chem. Eng. Japan, **13**, 397 (1980).
10) T. Murase, N. Hayashi, H. Suzuki and M. Shirato, "Two-dimensional Expression on Cylindrical Filter Element", Kagaku Kogaku Ronbunshu, **9**, 549 (1983).
11) M. Shirato, M. Iwata, M. Wakita, T. Murase and N. Hayashi, "Constant-Rate Consolidation Process of Semi-Solid Materials", Preprints of 51st Annual Meeting of SCEJ, F302 (1986).
12) M. Shirato, H. Kato, K. Kobayashi and H. Sakazaki, "Analysis of Settling of Thick Slurries due to Consolidation", J. Chem. Eng. Japan, **3**, 98 (1970).
13) M. Shirato, T. Murase, H. Doi and H. Shimaoka, "Analysis of Filtration Processes in Plate-and-Frame Press", Kagaku Kōgaku, **36**, 781 (1972).
14) M. Shirato, T. Murase, E. Iritani, M. Iwata and J. H. Cho, "Deliquoring by Expression due to Changing Filtrate Flow Pattern", Filtration & Separation, **22**, 250 (1985).
15) M. Shirato, T. Murase, M. Negawa and T. Senda, "Fundamental Studies of Expression under Variable Pressure", J. Chem. Eng. Japan, **3**, 105 (1970).
16) K. Terzaghi, "Theoretical Soil Mechanics", John Wiley & Sons, New York (1948).
17) M. Mikasa, "Nanjaku Nendo no Atsumitsu", Kashima Shuppankai, Tokyo (1963).

18) S. Okamura and M. Shirato, "Liquid Pressure Distribution within Cakes in the Constant Pressure Filtration", Kagaku Kōgaku, **19**, 104 (1955).
19) E. M. de Jager, M. van den Tempel and P. de Bruyne, "Permeability of Plastic Disperse Systems", Proc. Royal Aca. Amsterdam, Series B66, **1**, 17 (1963).
20) M. Shirato, T. Murase, M. Negawa and H. Moridera, "Analysis of Expression Operations", J. Chem. Eng. Japan, **4**, 263 (1971).
21) Y. Ishii, S. Kurata and T. Fujishita, "Reseaches on the Engineering Properties of Alluvial Clays", Trans. Japan Soc. Civil Eng., No. 30, 1 (1955).
22) B. Shivaram and P. K. Swamee, "A Computational Method for Consolidation-Coefficient", J. Japanese Soc. Soil Mech. Found. Eng., **17**, 48 (1977).
23) H. S. Carslaw and J. C. Jaeger, "Conduction of Heat in Solids", 2nd ed., Oxford, 102 (1958).
24) M. Shirato, M. Sambuichi, H. Kato and T. Aragaki, "Flow Variation through Constant Pressure Filter Cake", Kagaku Kōgaku, **31**, 359 (1967).
25) M. Shirato, H. Kato, T. Murase and M. Shibata, "Studies on Expression—Fundamental Analysis for Mechanism of Dehydration by Expression", J. Fermentation Technology (Japan), **43**, 255 (1965).